The oceanic zone of convergence on the eastern edge of the Pacific warm pool: A synthesis of results and implications for El Niño-Southern Oscillation and biogeochemical phenomena

Joel Picaut, Mansour Ioualalen, Thierry Delcroix, François Masia, Ragu Murtugudde, Jérome Vialard

▶ **To cite this version:**

Joel Picaut, Mansour Ioualalen, Thierry Delcroix, François Masia, Ragu Murtugudde, et al.. The oceanic zone of convergence on the eastern edge of the Pacific warm pool: A synthesis of results and implications for El Niño-Southern Oscillation and biogeochemical phenomena. Journal of Geophysical Research, 2001, 106, pp.2363-2386. 10.1029/2000JC900141 . hal-00772143

HAL Id: hal-00772143
https://hal.science/hal-00772143

Submitted on 11 Jan 2021

HAL is a multi-disciplinary open access archive for the deposit and dissemination of scientific research documents, whether they are published or not. The documents may come from teaching and research institutions in France or abroad, or from public or private research centers.

L'archive ouverte pluridisciplinaire **HAL**, est destinée au dépôt et à la diffusion de documents scientifiques de niveau recherche, publiés ou non, émanant des établissements d'enseignement et de recherche français ou étrangers, des laboratoires publics ou privés.

JOURNAL OF GEOPHYSICAL RESEARCH, VOL. 106, NO. C2, PAGES 2363–2386, FEBRUARY 15, 2001

The oceanic zone of convergence on the eastern edge of the Pacific warm pool: A synthesis of results and implications for El Niño-Southern Oscillation and biogeochemical phenomena

Joel Picaut,[1] Mansour Ioualalen,[2] Thierry Delcroix,[2] François Masia,[2] Ragu Murtugudde,[3] and Jérome Vialard[4]

Abstract. The eastern edge of the western Pacific warm pool corresponds to the separation between the warm, rainfall-induced low-salinity waters of the warm pool and the cold, high-salinity upwelled waters of the cold tongue in the central-eastern equatorial Pacific. Although not well defined in sea surface temperature (SST), this eastern edge is characterized by a sharp salinity front that is trapped to the equator. Several studies, using numerous in situ and satellite data and three classes of ocean models, indicate that this front is the result of the zonal convergence of the western and central Pacific water masses into the eastern edge of the warm pool. This occurs through the frequent encounter of the eastward jets in the warm pool and the westward South Equatorial Current in the cold tongue. The notable and alternate variations of these wind-driven zonal currents are trapped to the equator and are chiefly interannual in the vicinity of the edge. Consequently, the Eastern Warm Pool Convergence Zone (EWPCZ) is subject to eastward or westward displacements over several thousands of kilometers along the equatorial band, in synchrony with the warm phase (El Niño) and the cold phase (La Niña) of the El Niño-Southern Oscillation (ENSO) phenomenon. Zonal advection appears to be the predominant mechanism for the ENSO displacements of the eastern edge of the warm and fresh pool. The existence of the EWPCZ and its ENSO displacements have significant effects on the physics of the tropical Pacific and on related biogeochemical phenomena. The EWPCZ is important for the formation of the barrier layer in the isothermal layer of the warm pool. Its zonal displacements control SST in the central equatorial Pacific, which in turn drives the surface winds and atmospheric convection (and vice versa). Hence the central equatorial Pacific is a key region for ENSO coupled interactions. All these findings from several studies and additional analyses lead to a revision of the delayed action oscillator theory of ENSO. The existence of the EWPCZ and its zonal displacements are also reasons for the ENSO variations in production and exchange of CO_2 with the atmosphere over the equatorial Pacific. The zone of one-dimensional convergence seems to congregate the world's most important tuna fishery in the western equatorial Pacific, and its displacements are likely the reason for this fishery to move zonally over thousands of kilometers in phase with ENSO.

[1]Institut de Recherche pour le Développement (IRD), Laboratoire d'Etudes en Géophysique et Océanographie Spatiale, Toulouse, France.

[2]IRD, Nouméa, New-Caledonia.

[3]Earth System Science Interdisciplinary Center, University of Maryland, College Park, Maryland.

[4]European Centre for Medium-range Weather Forecasts, Reading, England, United Kingdom.

Copyright 2001 by the American Geophysical Union.

Paper number 2000JC900141.
0148-0227/01/2000JC900141$09.00

1. Introduction

El Niño has been historically identified as the arrival of warm water in the eastern equatorial Pacific and along the coast of Ecuador and Peru. However, it is through the seminal work of *Bjerknes* [1969] that the El Niño oceanic signal was related to the Indo-Pacific atmospheric fluctuation known as the Southern Oscillation. Consequently, the scientific community became interested in the opposite phase named La Niña [*Philander,* 1990]. El Niño-Southern Oscillation (ENSO) is now considered a coupled ocean-atmosphere system

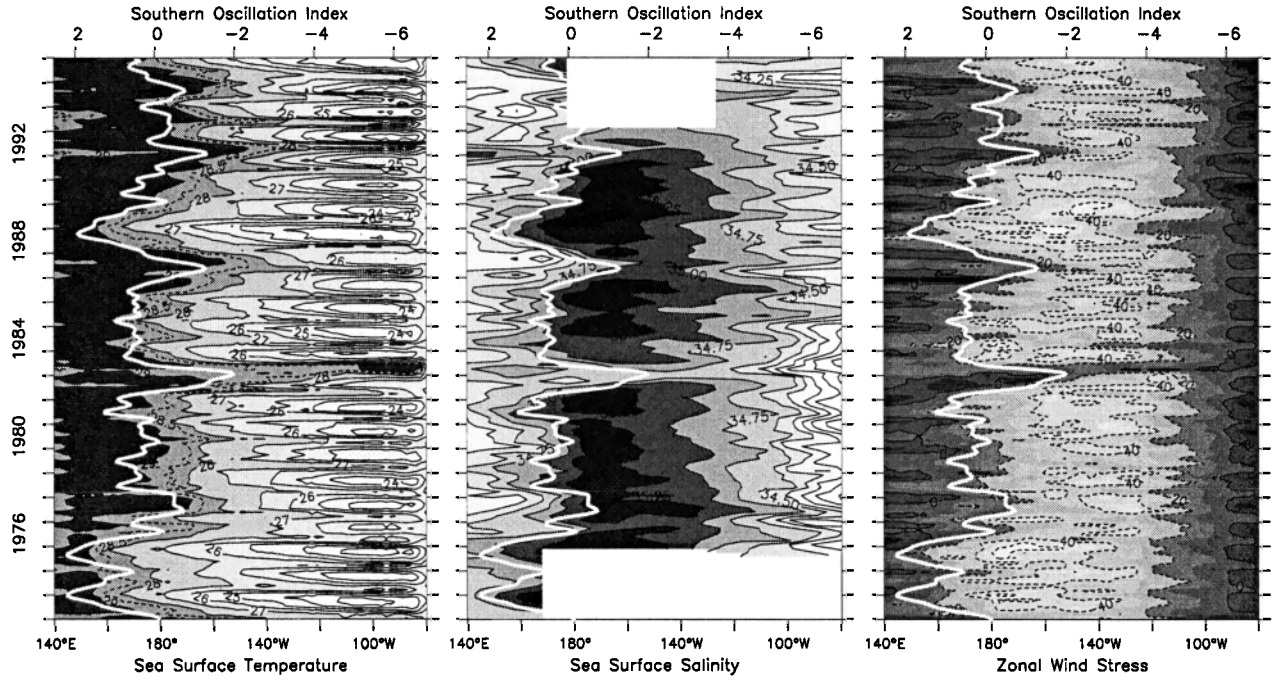

Figure 1. Longitude-time distribution of 4°N-4°S averaged (left panel) SST, (middle panel) sea surface salinity, and (right panel) pseudo zonal pseudo wind stress. Superimposed as a white thick line is the Southern Oscillation Index. Contours are 1°C, 0.25 psu, and 20 m^2 s^{-2} respectively.

composed of a warm phase (El Niño) and a cold phase (La Niña), which repeat irregularly every 2-7 years. As shown by the variations of the Southern Oscillation Index (SOI, Figure 1), the mean state does not stay for long. This mean state is characterized by a piling up of warm water in the western equatorial Pacific (the warm pool) by the South Equatorial Current (SEC) forced by the trade winds. Because of Ekman divergence, the trade winds generate an equatorial upwelling in the eastern part of the basin (the cold tongue). At the surface, the temperature gradient between the cold tongue and the warm pool drives the trade winds, completing the loop of the coupled ocean-atmosphere system. Underneath, the accumulation of warm water in the west and the upwelling in the east results in a thermocline that is deeper in the west and shallower in the east [*Lemasson and Piton,* 1968]. During a La Niña, which is to some extent an intensification of the mean state, the trade winds are stronger and result in an increase of the SEC and thus in a warm pool pushed toward the Philippine coasts. They also result in a stronger upwelling in the east, and overall, in a greater slope of the thermocline along the equator. During an El Niño, the trade winds relax or change direction with the occurrence of westerly wind bursts in the western equatorial Pacific. The accumulation of water in the warm pool is no longer balanced by the easterly wind stress. The warm water spreads toward the east in a surge led by downwelling equatorial Kelvin waves [*Wyrtki,* 1975]. The warm pool migrates eastward, while the equatorial Kelvin waves, on their fast way toward the east, push down the thermocline. In <2 months, these waves reach the eastern part of the equatorial basin and counteract the equatorial upwelling. The spreading of water masses to the center of the basin, as well as the reduced or annihilated upwelling in the east, flattens the slope of the thermocline along the equator [*Wyrtki,* 1984]. Consequently, the ENSO cycle appears as a seesaw of the thermocline along the equator accompanied by transfer of water mass and heat along the equator, which strongly affect the cold tongue and the warm pool.

In a study on the movements of the warm pool from satellite measurements, *Ho et al.* [1995] showed that it expands seasonally in the meridional direction roughly from 10° to 20° of latitude. *Schneider et al.* [1996] explained these meridional migrations by the seasonal variability of the net surface heat flux in each hemisphere. Interestingly, *Ho et al.* [1995] found that the dominant migration of the warm pool is on its eastern edge, in the zonal direction, within 7°N-7°S, and solely on the ENSO timescale. This was also noted by *Fu et al.* [1986], *Lukas and Webster* [1992] and *Picaut and Delcroix* [1995]. *Picaut and Delcroix* [1995] showed a striking resemblance between the phase of the SOI and the significant displacements (about 35° of longitude) of the eastern edge of the warm pool within 4°N-4°S, over the 1950-1994 period. They also found that these zonal displacements are barely affected by the seasonal cycle (an order of magnitude less than the interannual displacements). As shown by the superposition of the SOI (with reverse coordinate and scaled amplitude) over the sea surface temperature (SST) along the equatorial

Table 1. Correlation (Above the 95% Significance Level) Between the SOI and the Location of the Eastern Warm Pool Convergence Zone As defined by the 28°C, the 35-psu Isohaline, and the 20 m^2 s^{-2} Zonal Pseudo Wind Stress of Figure 1.[a]

	28°C	35 psu	20 m^2 s^{-2}
Time period	1961-1994	1976-1992	1961-1995
Correlation	-0.76	-0.78	-0.67

[a]adapted from *Delcroix* [1998].

band (Figure 1) and the correlation coefficient of Table 1, El Niño and La Niña are clearly defined by an eastward and westward migration, respectively, of the eastern edge of the warm pool. The migrations of this edge induce SST changes in the central equatorial Pacific around the 28°C threshold required for organized convection [*Gadgil et al.*, 1984; *Graham and Barnett*, 1987]. As a consequence, the convergence of winds over the Pacific warm pool associated with the convection and the ascending branch of the Walker circulation is also displaced zonally [*Fu et al.*, 1986; *Delcroix*, 1998]. This results during El Niño in the penetration and extent of the westerlies (associated with the East Asian winter monsoon and westerly wind events) into the central equatorial Pacific [*Wyrtki*, 1985; *Kessler et al.*, 1995; *Harrison and Larkin*, 1998]. On the other hand, during La Niña the easterlies, associated with the trades, penetrate from the central equatorial Pacific into the western Pacific. The movements of these zonal winds are illustrated in Figure 1 where the SOI curve matches quite well the 20 m^2 s^{-2} Florida State University (FSU) pseudo zonal wind stress isoline (Table 1).

In the western half of the equatorial Pacific, ENSO can therefore be seen as a zonal migration of the warm pool. ENSO appears also as a variation of temperature in the cold tongue. Two decades ago, it was found that remote forcing through equatorial Kelvin waves (and the consequent effect on the shallow thermocline) is responsible for the interannual variations of SST in the cold tongue [e.g., *Wyrtki*, 1975; *McCreary*, 1976]. Only recently has it shown that the migrations of the eastern edge of the warm pool are mainly due to zonal advection [*McPhaden and Picaut*, 1990; *Picaut and Delcroix*, 1995]. As noted above, these zonal migrations are clearly dominated by the interannual ENSO signal (Figure 1 and Table 1), unlike the cold tongue, which is also influenced by the seasonal signal. Hence, the interannual variations of SST in the central and eastern equatorial Pacific display very similar patterns, albeit driven mostly by different physics. During the course of the El Niño-La Niña events the convection zone over the warm pool and its associated precipitation follow the zonal migration of the eastern edge of the warm pool, as indicated by the movement of high reflective clouds [*Fu et al.*, 1986]. The heavy rainfall significantly reduces the salinity of the upper layer of the warm pool, which is the reason why the warm pool was also named the fresh pool [*Delcroix and Picaut*, 1998]. On the contrary, because of evaporation and equatorial upwelling, the cold tongue is composed of high salinity water. Recently, it was found that the water masses of these two regions converge zonally into a well-defined salinity front [*Picaut et al.*, 1996]. This convergence also leads to the formation of the barrier layer [*Lukas and Lindström*, 1991] in the isothermal layer of the warm pool [*Vialard and Delecluse*, 1998b]. Nearly coinciding in location, the zone of convergence, the salinity front, and the eastern edge of the warm pool, all migrate zonally with the phases of ENSO (Figure 1).

The present work was motivated by the Tropical Ocean - Global Atmosphere (TOGA) - Coupled Ocean-Atmosphere Response Experiment (COARE) international programme [*Webster and Lukas*, 1992]. Its main purpose is to synthesize recent results and additional analyses, which establish the existence of an oceanic zone of convergence at the eastern edge of the warm pool. Its purpose is also to discuss several of the important implications for ENSO, which have been mostly reported in previous studies. In addition to implying a revision to the delayed action oscillator theory for ENSO, the discovery of a zonal convergence zone, controlled by oceanic advection, has several implications for biogeochemical phenomena and consequently, tuna fisheries in the central and western Pacific, which are also reviewed herein. The existence and ENSO displacements of the oceanic zone of convergence are presented and discussed in sections 3 and 4. This is done through the analysis of a maximum of in situ and satellite data and the output from three different types of ocean model, which are first presented in section 2. Several consequences of this zone of convergence on the physics of ENSO are discussed: the ENSO coupling in the central equatorial Pacific, a revision of the delayed action oscillator theory of ENSO, and the transfer of mass and heat and ENSO memory. The amount of CO_2 released into the atmosphere from the cold tongue is dictated by the size of the cold tongue, hence by the location of the zone of convergence. Similarly, the ENSO variations of production are related to the extent of the zone of convergence separating the oligotrophic water of the warm pool from the eutrophic water of the cold tongue. The convergence of water masses into the eastern edge of the warm pool seems to congregate the most important tuna fishery of the world, and it could be the reason for the zonal displacements of this fishery over thousands of kilometers in phase with ENSO. All these consequences are summarized in section 5, which is followed by some general conclusions.

2. Means of Study

2.1. Data

The Tropical Atmosphere-Ocean (TAO) array is composed of about 70 buoys and covers most of the equa-

torial Pacific within 8°N-8°S, 95°W-137°E [*Hayes et al.*, 1991; *McPhaden*, 1993]. The studies and additional analyses that are synthesized here, used the near-surface salinity measured by the TAO array in the warm pool, as well as the near-surface (10-50 m depth) velocity taken at four equatorial sites located at 156°E, 165°E, 140°W, and 110°W. A 5 day zonal surface current field along the equator (referred to as the TAO field) over the 1986-1994 period was built from an objective analysis of the near-surface zonal currents at these four equatorial sites. Bearing in mind that the 156°E current data started only in August 1991 and that 30° is the zonal decorrelation scale of the zonal current at the equator for periods greater than 50 days [*McPhaden and Taft*, 1988; *Picaut et al.*, 1990], this TAO current field has to be used with some care.

Two other in situ current fields were also used. One is a mean climatology issued from a compilation of about 1500 near-surface drifting buoys during the 1987-1996 period within 20°N-20°S, 135°E-90°W and binned on a 2° latitude × 4° longitude grid. The other field results from a combination of all the near-surface drifting buoys and the near surface current measurements from the four TAO moorings at the equator. Using an objective analysis, bimonthly currents over the 1987-1993 period were mapped on a 1° latitude × 5° longitude grid between 20°N and 20°S and 120°E and 80°W. Information on the processing and validation are detailed by *Reverdin et al.* [1994] and *Frankignoul et al.* [1996]. Despite an increase in the number of drifting buoys after mid-1988, this bimonthly current field must also be used with some care because of its coarse sampling. Even if this field includes some TAO current data, it will be referred to as the "buoy field"in the following to avoid any confusion with the "TAO field"of the zonal current derived exclusively from moored current observations.

The Geosat anomalous zonal current field was obtained from the analysis of *Delcroix et al.* [1994]. The original Geosat geophysical data records used improved satellite orbit and water vapor corrections [*Cheney et al.*, 1991]. It was transformed into sea level anomaly relative to the first 2 years of the Exact Repeat Mission in order to remove the imprecise geoid along the repetitive tracks. Various filtering and gridding procedures resulted in a sea level anomaly field on a 0.5° latitude, 5° longitude and 5 day grid from November 1986 to March 1989 and between 28.5°S and 28.5°N and 125°E and 85°W. A low-pass-filtered (35 day Hanning filter) zonal current anomaly field was built from the second meridional derivative of the sea level at the equator and the first derivative away from the equator following the techniques discussed by *Picaut et al.* [1990] and *Picaut and Tournier* [1991]. It was validated against the near-surface current measurements at the equator and at 165°E, 140°W, and 110°W with correlations of 0.92, 0.70, and 0.49 and rms differences of 17, 24, and 31 cm s^{-1}, respectively. The total zonal current along the equatorial band needed for the present study was built from the sum of the previous zonal current anomalies relative to the 1987-1988 period and the mean of the TAO field over the same period. Following *Picaut and Delcroix* [1995], a conversion factor of 0.75 was used to extrapolate these zonal currents along the equator to the 4°N-4°S band.

The TOPEX/Poseidon zonal current field was built from the original along-track sea level data taken from the CD-ROMs generated at Collecte Localisation Satellite (CLS) as part of the AVISO/Altimetry programme. The low-pass filtered zonal current anomaly field (relative to the September 1992 to October 1996 period) was built following the same technique as in the previous Geosat current field; details are given by *Delcroix et al.* [2000]. Comparison with the near-surface zonal current measurements at the equator and at 156°E, 165°E, 140°W, and 110°W resulted in a correlation of 0.86, 0.90, 0.58, and 0.45 and a rms difference of 15, 16, 33, and 38 cm s$^-$1, respectively. Of most interest for the present study, the Geosat and TOPEX/Poseidon-derived surface zonal currents are fairly representative of the observed near-surface currents within a region encompassing the western and eastern limits of the eastern edge of the warm pool.

Additional data have been used in the analyses. Two monthly SST data sets came from the National Centers for Environmental Prediction (NCEP). One is a combination of ship, buoy, satellite data, and it covers the period from January 1985 to present [*Reynolds and Smith*, 1994]. The other, based mostly on in situ data, covers the 1950-1992 period [*Smith et al.*, 1996]. About 16,000 sea surface salinity (SSS) data were collected in the 4°N-4°S equatorial band from 1973 to 1995. Most of them came from the Institut de Recherche pour le Développement (IRD, former ORSTOM) Voluntary Observing Ship program (bucket, and since 1992, thermosalinograph), which covers essentially four major cross-equatorial routes. Details about validation and gridding procedure are given by *Delcroix* [1998]. Along the 165°E cross-equatorial section, 42 cruises have been carried out, mostly during the TOGA programme. The processing of the vertical profiles of salinity and current into a regular grid is detailed by *Delcroix et al.* [1992]. Surface wind stress is also considered and it was obtained from the 2° × 2° FSU pseudo wind stress product [*Legler and O'Brien*, 1984].

2.2. Models

The first model is linear and forced by observed wind-stress field over the 1961-1992 period [*Cane and Patton*, 1984]. The linear shallow-water equations are solved on an equatorial β plane, subject to the low-frequency and longwave approximations. Variables are calculated every 5 days on a staggered grid of 2° longitude by 0.5° latitude. The model basin is bounded at 130°E and 80°W, 20°N and 20°S, and the coast of Central America and of Papua New Guinea-Australia are approximated by two rectangles [*du Penhoat et al.*, 1992].

The forcing is derived from the FSU monthly pseudo stress wind product through a constant drag coefficient C_D and is then linearly interpolated to the model time and space grid. These solutions are generated for the first 10 vertical modes calculated from a specific vertical density profile. The total sea level height field is found by summing the individual contribution of these modes. Following *Zebiak and Cane* [1987], a shallow frictional layer of constant depth is added to simulate the surface intensification of wind-driven currents in the real ocean. Model wind stress projections and internal wave speeds are calculated from several types of vertical density profiles. A mean profile representative of the central-western Pacific is generally used. Two other mean profiles representative of the eastern and western equatorial Pacific are also used to test the sensitivity of the model to the choice of profile.

Of the two Ocean General Circulation Models (OGCMs) used in the analyses, one is a reduced gravity, primitive equation OGCM [*Gent and Cane,* 1989; herein referred to as GC] that was specifically designed for upper tropical ocean simulations. This model is vertically divided into a specified number of layers (20 in the present study). The uppermost layer represents the mixed layer and the layers below are chosen according to a sigma coordinate. Once the depth of the mixed layer and the depth of the last sigma layer are predicted, the thickness of the remaining layers is calculated diagnostically. The mixed layer physics that determines the mixed layer depth is based on the hybrid vertical scheme developed by *Chen et al.* [1994]. Another important model component is the formulation of surface heat fluxes. The ocean model is coupled to an advective atmospheric mixed layer model [*Seager et al.,* 1995]. With this model the complete heat flux can be computed with only solar radiation, cloud cover and winds needing to be externally specified. This formulation significantly improves the ocean model performance [*Murtugudde and Busalacchi,* 1998]. The wind stress and wind speed were derived from the FSU pseudo wind stress data set. For the freshwater flux the Climate-Prediction-Center Merged Analysis of Precipitation (CMAP) data set [*Xie and Arkin,* 1996] over the January 1979 to July 1999 period was used. A seasonal precipitation climatology was derived from the CMAP data set.

An OGCM, developed at Laboratoire d'Océanographie DYnamique et de Climatologie (LODYC) [*Delecluse et al.,* 1993], has also been used to study zonal advection in the central-western equatorial Pacific. A first version of the OPA model covers the tropical Pacific Ocean within 30°N-30°S, 130°E-75°W [*Maes et al.,* 1997; *Vialard and Delecluse,* 1998a]. It has a zonal resolution of 1°, a meridional resolution variable from 1/2° near the equator to 2° at the poleward boundaries, and a vertical resolution (20 layers) variable from 10 m in the upper 120 m to 1000 m at depth. The second version of the model [*Maes et al.,* 1998] covers the three tropical oceans between 50°N and 50°S with a higher resolution, i.e., 30 layers in the vertical and 1/3° in latitude and longitude near the equator and near the coasts. Vertical mixing coefficients are computed through a turbulent kinetic energy closure model [*Blanke and Delecluse,* 1993]. The external forcing (wind stress, freshwater flux, and net heat flux) is provided by the Meteo-France Atmospheric General Circulation Model (AGCM) ARPEGE forced by the Reynolds' observed SST over the 1985-1994 period [*Vialard and Delecluse,* 1998a]. The heat flux from the AGCM might not be in equilibrium with the model dynamics. A restoring term (with a restoring coefficient of 40 W m^{-2} $°C^{-1}$) toward the observed SST is added in order to avoid unrealistic temperatures. This parametrization approximates at the zero order the strong coupling between the oceanic heat losses and the SST.

Table 2. Correlation (C) Between the Simulated Surface Zonal Currents From the Three Ocean Models (Linear, OPA, and GC) and the Observed Near-Surface Zonal Currents From the Three TAO Equatorial Moorings.[b]

x/y	C(x/y)	$\bar{x}$	$\bar{y}$	sd(x)	sd(y)
GC/TAO-110°W	0.47	-19	-10	36	33
OPA/TAO-110°W	0.54	-32	-10	38	33
Lin-10/TAO-140°W	0.30	-65	-15	38	27
OPA/TAO-140°W	0.35	-40	-15	32	27
GC/TAO-140°W	0.41	-4	-15	31	27
Lin-01/TAO-165°E	0.34	4	-2	29	32
Lin-10/TAO-165°E	0.48	-2	-2	38	32
OPA/TAO-165°E	0.39	7	-2	36	32
GC/TAO-165°E	0.60	11	-2	37	32

[b]The results of the linear model are shown for 1 and 10 vertical modes. Also listed are the mean zonal currents (bar) in cm s^{-1} and their standard deviations (sd) in cm s^{-1}. Only correlations higher than the 95% significance level are shown.

A comparison with the observed monthly zonal currents at three TAO equatorial sites is presented (Table 2) in order to assess the relevance of simulated currents along the equator. With different wind forcing and, for the OGCMs, two different approaches for heat and freshwater fluxes this comparison cannot be used for model intercomparison. There is an improvement in the linear model when using 10 vertical modes instead of the first mode. The modeled zonal surface currents in the west are approaching the observations, in particular, a weak mean eastward flow. However, the linear model is quite deficient in the central-eastern equator, with a stronger westward mean flow and a poor simulation of its variability. As expected, the two OGCMs behave better in this region. The variabilities are close to the observed one, but the westward flow is strong in OPA. In the warm pool the two OGCMs behave correctly in simulating the surface zonal current at the equator, but

they are not much better than the linear model with 10 vertical modes.

3. Zonal Displacements of the Eastern Edge of the Warm Pool

Wyrtki [1975, 1985] was the very first to recognize the importance of the zonal migration of the warm pool in relation to El Niño, and *Gill* [1983] suggested that this migration is mostly due to advection by zonal current anomalies. *Gill* [1983] also suggested looking at the displacement of water mass by the zonal current averaged over the equatorial waveguide. The use of hypothetical drifters with a huge drogue has the advantage of following the water masses along the equatorial waveguide. On the contrary, real drifters would sooner or later escape the equatorial band with, in particular, the divergence associated with the equatorial upwelling. This technique was successfully applied in several studies, such as by *Picaut et al.* [1996]. It will be used and fully justified in the following sections.

3.1. Observational Results

The technique is illustrated on Figure 2 with two hypothetical drifters with a 4°N-4°S drogue launched into the zonal surface current anomalies derived from Geosat altimetry measurement over the November 1986 to February 1989 period (Figure 2, upper panel). During the 1986-1987 El Niño the drifters move toward the east with the dominant eastward currents, while they move toward the west during the 1988-1989 La Niña. When the trajectories of these two drifters are superimposed on the observed SST averaged within the same 4°N-4°S equatorial band (Figure 2, middle panel) they bracket the eastern edge of the warm pool. With the zonal SST gradient on the edge nearly constant this reflects that zonal advection is the dominant mechanism for the 1986-1989 El Niño-La Niña zonal migrations of the eastern edge of the warm pool [*Picaut and Delcroix,* 1995].

Because of the uncertainty in the determination of the mean geoid, altimetry derived currents are relative to some mean. The addition of the zonal mean current derived from the TAO field results in a remarkable feature (Figure 2, lower panel). After about 1 year the two hypothetical drifters converge into a single trajectory, which follows the retreat of the warm pool associated with the 1988-1989 La Niña event [*McPhaden and Picaut,* 1990] and finally reaches the western limit of the current field. The convergence of the two trajectories is due to the mean zonal currents along the equator, composed of a weak mean eastward flow in the warm pool and a significant mean westward flow in the cold tongue that converge into a position close to the dateline.

As discussed by *Delcroix et al.* [2000] over the 1992-1998 period the use of surface current derived from TOPEX/Poseidon leads to similar results (Figure 3).

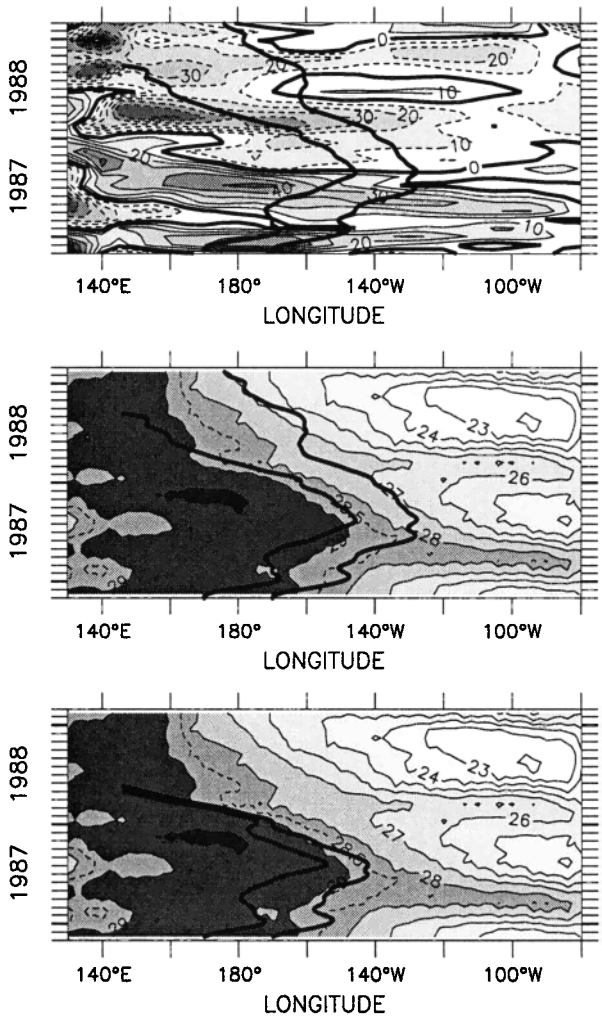

Figure 2. Trajectories of hypothetical drifters moved by surface zonal currents derived from Geosat and averaged within 4°N-4°S: (upper panel) currents anomalies relative to 1987-1988, (middle panel) currents anomalies superimposed on the observed SST, and (lower panel) total currents superimposed on the observed SST. Contours are 10 cm s^{-1} and 1°C respectively.

During the 1993-1994 El Niño events and the beginning of the 1995-1996 La Niña the trajectories of the two hypothetical drifters displaced by the 2°N-2°S current anomalies (Figure 3, left panel), bracket the displacement of the eastern edge of the warm pool (as inferred from Figure 3, right panel). Similar to what happened during the 1988-1989 La Niña (Figure 2), the trajectories reach the western limit of altimetry-derived currents during the 1995-1996 La Niña. Other drifters launched in spring 1996 are drastically moved eastward by the anomalous eastward flow associated with the 1997 El Niño. The use of the total currents (Figure 3, middle panel) results in a convergence of the hypothetical drifters into a single trajectory near the eastern edge of the warm pool during the successive 1992-1994 El Niño events (Figure 3, right panel). During the

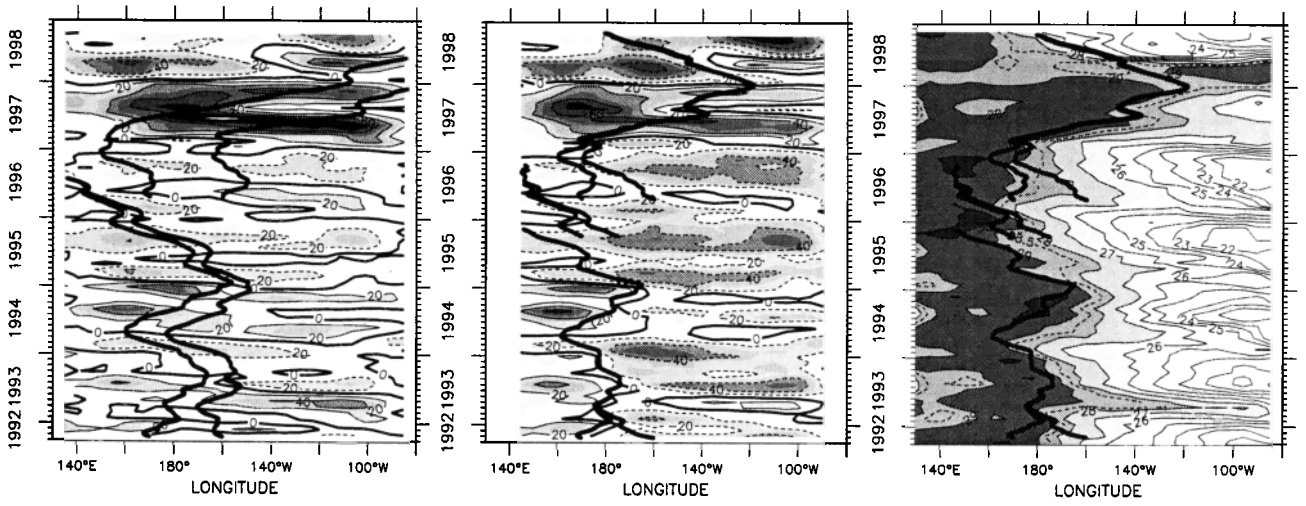

Figure 3. Trajectories of hypothetical drifters moved by surface zonal currents derived from TOPEX/Poseidon and averaged within 2°N-2°S: (left panel) currents anomalies relative to September 1992-October 1996, (middle panel) total currents, and (right panel) total currents superimposed on the observed SST. Contours are 20 cm s^{-1} and 1°C respectively.

1995-1996 La Niña all the drifters are pushed into the western limit of the current field. By the end of 1996 the total current becomes eastward, and the drifters are then pushed by the powerful 1997 El Niño eastward surface flow. The zone of convergence is not so well defined during this strong El Niño. However, a single trajectory appears close to the 29°C during the warm event and then underlines the retreat of the warm pool associated with the 1998 La Niña.

Most of the hypothetical drifters launched in early 1988 in the western equatorial Pacific into the bimonthly buoy field have a tendency to converge into a single trajectory after 2 years (Figure 4). Then they roughly follow the migration of the eastern edge of the warm pool, although with a westward offset that may be due to the strong smoothing of the current field. All the drifters launched east of the edge reach rapidly the common trajectory, due to the dominance of the westward flow in the central-eastern equatorial Pacific [*Reverdin et al.*, 1994]. This is illustrated by one drifter launched at 160°W at the end of 1990. On the other hand, drifters launched in the far western equatorial Pacific do not necessarily reach the common trajectory. In the warm pool, the mean eastward current is not well defined and sometimes not strong enough to counteract sporadic westward currents.

Using the TAO field (Figure 5), the trajectory of the drifters launched in 1986 follows the eastern edge of the warm pool, except during the 1988-1989 La Niña, when it is interrupted as it passes the westernmost TAO site at 156°E. Three drifters are launched farther east in 1990. They converge into a single trajectory after 2-3 years and then closely follow the migration of the eastern edge of the warm pool associated with the 1991-1992 and 1992-1993 El Niño events.

These results from four different sets of observations exhibit similar features. Because of the presence of mean zonal converging currents, the water masses along the equator meet at a zone of confluence, or one-dimensional convergence. This zone happens to be situated close to the eastern edge of the warm pool (i.e., the 29°C isotherm) and migrates eastward and westward with this edge during El Niño and La Niña, respectively. This zone is easily evidenced by the trajectories

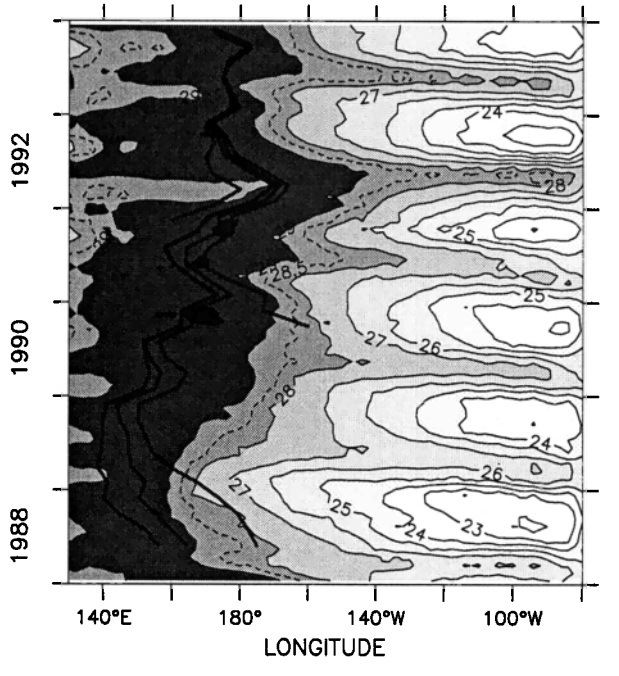

Figure 4. Trajectories of hypothetical drifters moved by near-surface zonal currents issued from the buoy field and averaged within 4°N-4°S. Superimposed is the observed SST (contour every 1°C).

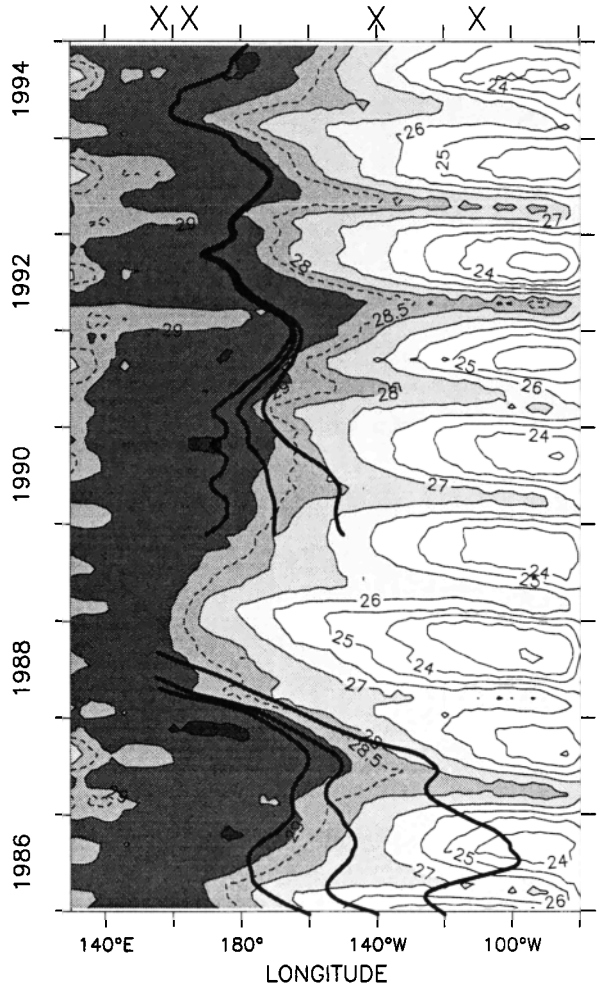

Figure 5. Trajectories of hypothetical drifters moved by near-surface zonal currents issued from the TAO field along the equator. The crosses denote the location of the equatorial moorings used to build the TAO field. Superimposed is the observed SST (contour every 1°C).

of hypothetical drifters launched in the east as the dominance of westward flow along the equator would always push the drifter into the eastern edge of the warm pool. On the other hand, the zonal current in the equatorial band of the warm pool is weakly eastward on a mean but it can be subject to strong eastward intraseasonal and interannual variations [e.g., *McPhaden et al.*, 1992; *Frankignoul et al.*, 1996]. As a consequence, the western side of the oceanic zone of convergence is not so well defined, and it can be pushed eastward past the eastern edge of the warm pool during the 1988-1989 and 1995-1996 La Niña events.

3.2. Modeling Results

The linear model does not include an SST equation. Hence the hypothetical drifter trajectories moved by the <4°N-4°S> simulated zonal currents are superimposed over the observed SST averaged within the same band (Figure 6). All the hypothetical drifters launched in the eastern equatorial Pacific reached the oceanic zone of convergence as defined by the single trajectory within 2-4 years. Similar to observations, almost all of the drifters launched within 10° west of this convergence zone reached it after a year or 2. Over the first half of the 1961-1992 period of model run the unique trajectory seems to follow the zonal migration of the other side of the warm pool as defined by the 29°C contour. During the second half the trajectory remains in the middle of the warm pool, and it is subject to strong zonal migrations that are in phase with those of the eastern edge of the warm pool. At the same time the warm pool seems to expand zonally. The long-term change of the position of the zone of convergence is due to a modification in the strength of the converging currents along the equator. It is tempting to relate these simultaneous changes to those around 1976 in the frequency of ENSO events and in the subsurface temperature, associated with long-term and decadal variations [*Trenberth and Hoar*, 1996; *Guilderson and Schrag*, 1998; *Lau and*

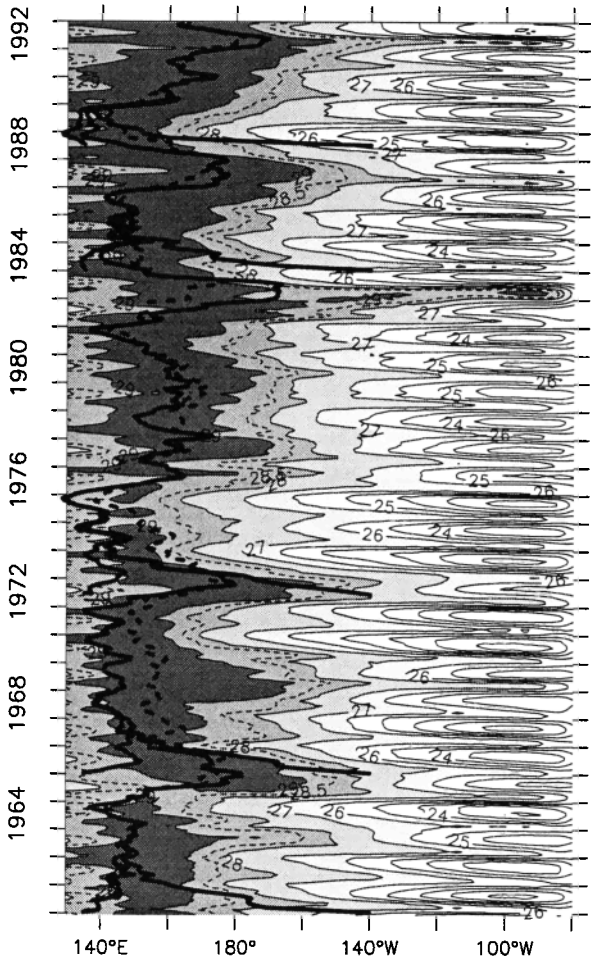

Figure 6. Trajectories of hypothetical drifters moved by surface zonal currents issued from the linear model and averaged within 4°N-4°S. Superimposed is the observed SST (contour every 1°C). The dashed (full) line corresponds to the model run with the first (10) vertical mode(s).

Weng, 1999]. Such changes are beyond the scope of the present study, especially knowing the simplicity of the model used and the uncertainties in the determination of the 29°C position from scattered in situ SST observations prior to the use of satellite sensors [*Smith et al.,* 1996].

The lack of nonlinear terms in this model is likely the reason for the zone of convergence to be situated too much into the warm pool as compared to observations and the following OGCMs' results since nonlinearities strengthen the eastward equatorial currents and weaken the westward equatorial currents [*Philander and Pacanowski,* 1980]. Other parameters of the linear model may be responsible for the westward shift of the mean position of the zone of convergence. As shown on Figure 6, the use of just the first vertical mode reduces this shift and also the amplitude of the ENSO migrations of the zone of convergence. An increase in the Rayleigh friction coefficient from 2.5 year^{-1} to 6 month^{-1} results in a 30% reduction of the El Niño eastward migrations and, therefore, on average in an increase of the westward shift. The ENSO migrations of the single trajectory are not much affected by the change of the drag coefficient within the range 1-2 × 10^{-3}. Similarly, there are no significant changes in the position of the convergence zone with the replacement of the mean vertical density profile used in this model by one representative of the cold tongue or another representative of the warm pool. Only a significant increase of the mixed layer (from 43 to 70 m) will shift the mean position of the zone of convergence eastward by about 10°. All these tests indicate that despite the limitation of the simulated currents the zone of convergence, its ENSO migrations, and its westward shift inside the warm pool are intrinsic and permanent features of the linear model.

The OPA OGCM simulates SST; hence this field can be used in conjunction with the simulated current field. The trajectory of a hypothetical drifter with a 4°N-4°S drogue follows the migration of the eastern edge of the warm pool defined by the 29°C isotherm (Figure 7). A discrepancy appears in the boreal summer of 1993 where the drifter is moving in the opposite direction to the eastward expansion of the warm pool associated with the 1993 El Niño. The trajectory is unique, except briefly during the peak of the 1988-1989 La Niña. Other drifters on Figure 7 illustrate the existence of the oceanic zone of convergence close to the eastern edge of the warm pool. The zone of convergence is emphasized by the superposition of the trajectories on the simulated

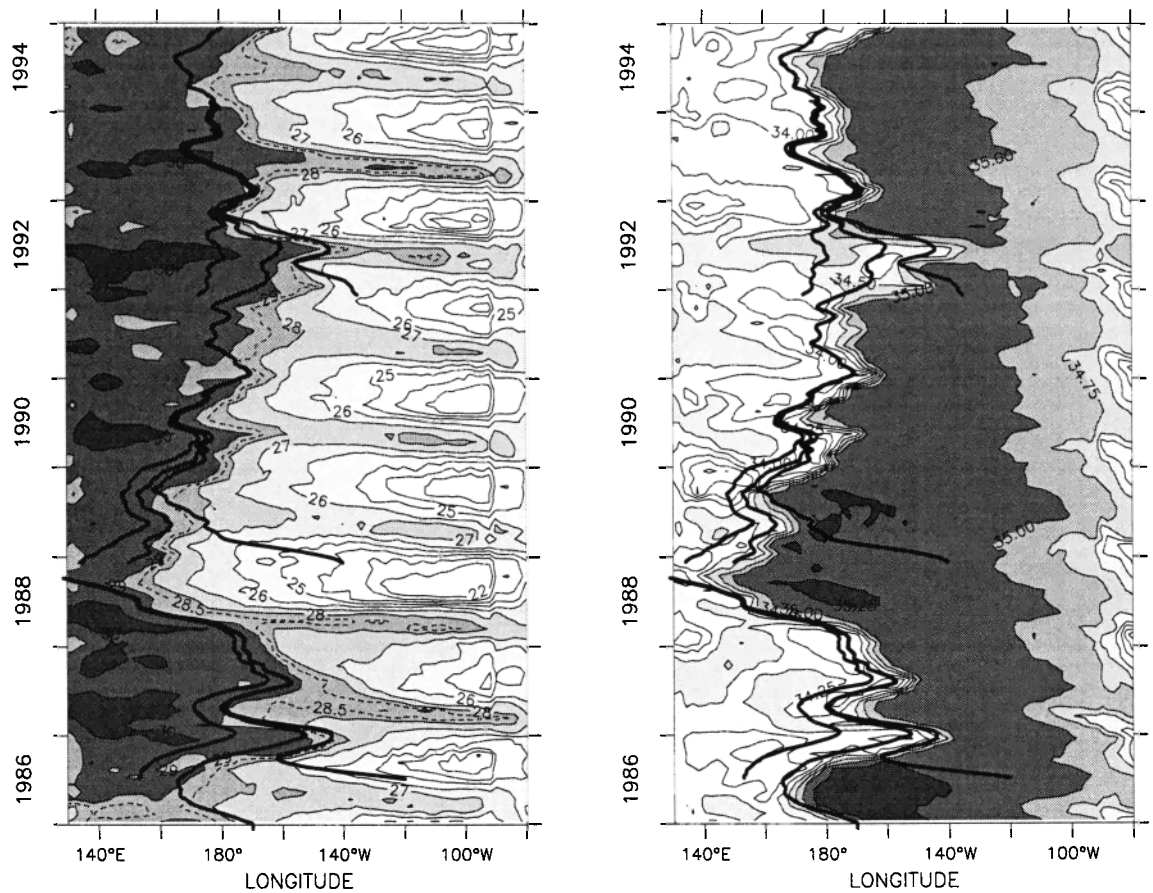

Figure 7. Trajectories of hypothetical drifters moved by the surface zonal currents issued from the OPA model and averaged within 4°N-4°S. Superimposed is (left panel) the SST and (right panel) the SSS. Contours are 1°C and 0.25 psu respectively.

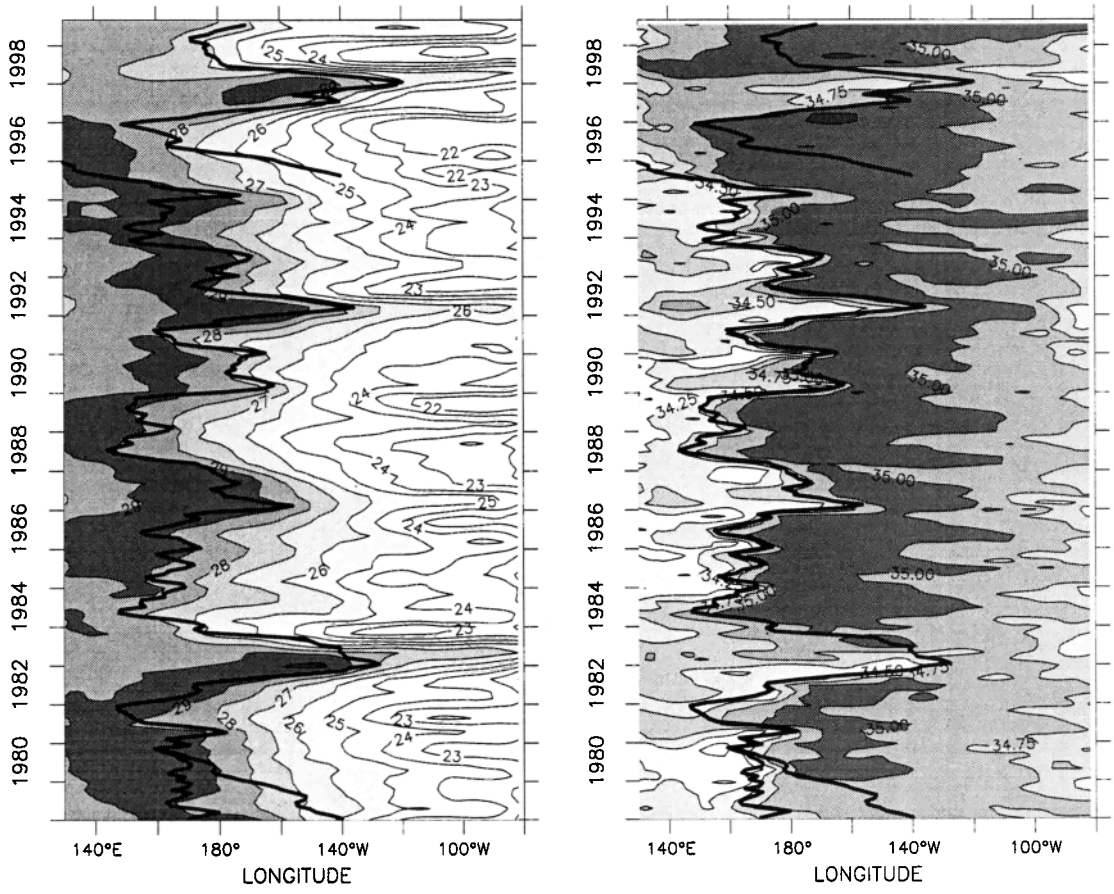

Figure 8. Trajectories of hypothetical drifters moved by the surface zonal currents issued from the GC model and averaged within 2°N-2°S. Superimposed is (left panel) the SST (right panel) the SSS. Contours are 1°C and 0.25 psu respectively.

SSS field. Because of evaporation and the presence of the equatorial upwelling, which brings high-salinity water from below, the surface water of the central equatorial Pacific is characterized by relatively cold temperature and high salinity. On the other hand, the heavy precipitation that moves in synchrony with the warm pool results in low surface salinity in the west. As shown on Figure 7, these very different water masses meet on the eastern edge of the warm pool in a single drifter trajectory and result in a sharp SSS front that moves zonally with the ENSO phases. This front is aligned meridionally, and it appears to be trapped to the equator. Interestingly, the displacement of the simulated salinity front matches almost every detail of the single trajectory. *Maes et al.* [1998] first simulated this front with the OPA model, and *Vialard and Delecluse* [1998b] discussed it in detail with the same model. This front and its displacements bear much resemblance to those deduced from merchant ship SSS observations (Figure 1).

The results with the GC model forced by the CMAP precipitation data set over the January 1979-July 1999 period are first presented (Figure 8). The trajectory of a hypothetical drifter with a 2°N-2°S drogue mostly follows the migrations of the eastern edge warm pool defined by the 29°C isotherm. The trajectory is unique from 1979 until the 1995-1996 La Niña, where it reaches the western side of the basin. In early 1996 a drifter launched at 140°W is first pushed toward the west, and with the start of El Niño it follows the huge eastward migration of the warm pool associated with this powerful event. Similar to the results with the TOPEX/Poseidon-derived current, the retreat of the warm pool associated with the rapid shift into the 1998 La Niña is captured by the hypothetical drifter. The convergence of the water masses on the eastern edge of the warm pool is highlighted by a salinity front, on the same way as the OPA simulation.

Another run was done with the GC model forced by the CMAP seasonal climatological freshwater flux (not shown). As expected, the salinity contrast between the central and western equatorial Pacific is reduced by about 0.5 psu and so is the strength of the salinity front. This change of freshwater flux has little impact on the simulated surface currents. The position of the zone of convergence defined by the drifter trajectory is almost unchanged, and the salinity front remained attached to this zone of convergence in the same way as the previous

run with the 1979-1999 CMAP precipitation (Figure 8). Differences in freshwater fluxes clearly alter simulated SSS [e.g., *Yang et al.,* 1999], and the ARPEGE-AGCM freshwater flux used in the OPA-OGCM has several deficiencies compared to observations [*Vialard and Delecluse,* 1998a]. However, the results with these two OGCMs, and, in particular, the last test with a climatological precipitation, assert the robustness of the present analysis: the zone of one-dimensional convergence on the eastern edge of the warm pool is marked by a salinity front, which is displaced with the eastern edge of the warm pool in phase with ENSO. The precipitation and evaporation are needed to build the salinity front, but like the SST on the eastern edge of the warm pool, the zonal displacements of this salinity front are mainly driven by the surface zonal currents within the equatorial band.

4. Discussion

4.1. Zonal Advection

Near-surface zonal current fields along the equatorial band, deduced from four different types of in situ and satellite observations and from three classes of ocean model, have evidenced the existence of an oceanic zone of convergence on the eastern edge of the warm pool. This zone of one-dimensional convergence, the Eastern Warm Pool Convergence Zone (EWPCZ), moves back and forth along the equator in synchrony with the phases of ENSO. The EWPCZ was evidenced through the use of hypothetical drifters with a drogue covering the equatorial band that integrates the variation in time and space of the zonal currents in this band. The oceanic zone of convergence is tracked down by Lagrangian drifters, and since the SST gradient on its east is oftentimes nearly constant (Figure 1), this implies that zonal advection is the dominant mechanism for the ENSO displacement of the eastern edge of the warm pool. This is in agreement with the Lagrangian approaches of *Gill* [1983], *McPhaden and Picaut* [1990] and *Picaut and Delcroix* [1995], in particular, with a verification in the equation governing the equation of heat by *Picaut and Delcroix* [1995]. This has been further confirmed by recent modeling and observing studies in the central-western equatorial Pacific using a Eulerian approach [e.g., *Perigaud and Dewitte,* 1996; *Vialard et al.,* 2000; *Wang and McPhaden,* 2000]. Hence it is not surprising that *Liu et al.* [1994] were unable to find a dependence between SST tendency and atmospheric heat flux in the central equatorial Pacific.

Section 3 also shows that the EWPCZ is marked by a salinity front. The SSS field of Figure 1 was built mostly from merchant ship observations, which mainly cover four main and large cross-equatorial sections [*Delcroix et al.,* 1996]. The interpolation within these sections underestimates the strength of the salinity front. Numerous salinity observations taken from research vessel sections along the equator [e.g., *Mangum et al.,* 1990; *Kuroda and McPhaden,* 1993; *Inoue et al.,* 1996; *Eldin et al.,* 1997], from TAO mooring [e.g., *McPhaden et al.,* 1992; *Sprintall and McPhaden,* 1994], and from thermosalinograph onboard merchant ships [e.g., *Hénin and*

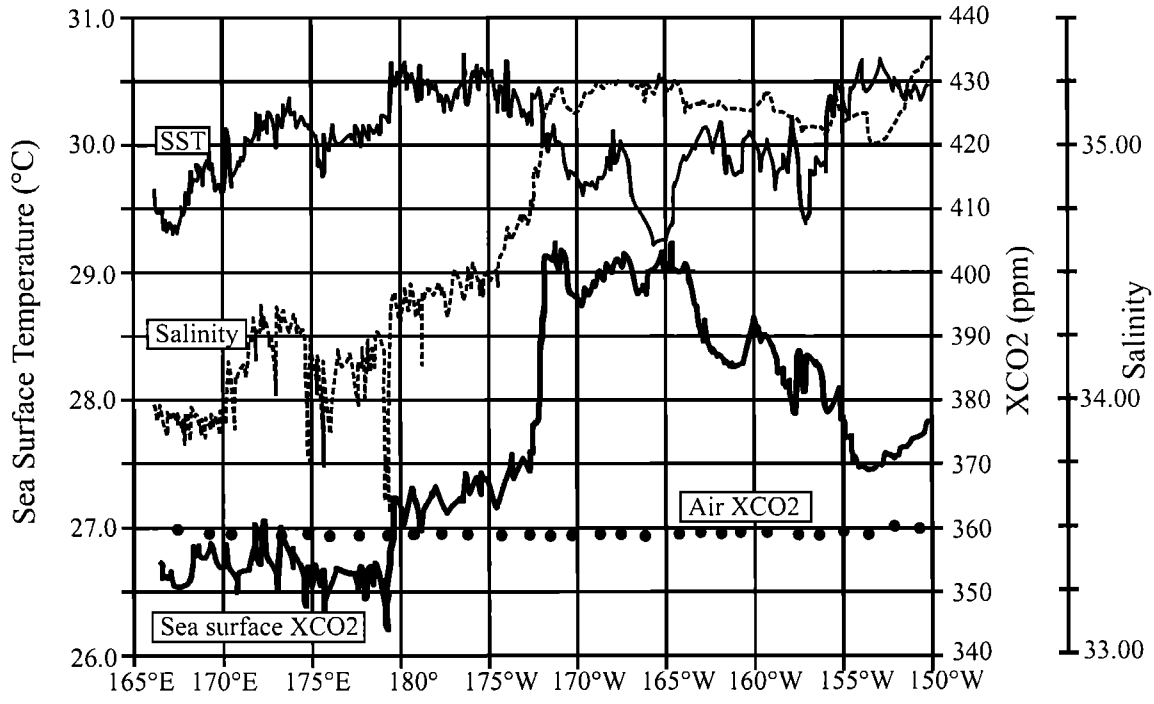

Figure 9. Continuous surface measurements along the equator during the Flupac cruise in October 1994: SST, SSS and sea surface CO_2 concentration [from *Le Borgne et al.,* 1995].

Grelet, 1996; *Hénin et al.,* 1998] confirm that this salinity front is a common feature of the eastern edge of the warm pool and indicate that it can be quite tight. This is illustrated on Figure 9 taken from continuous surface measurements along the equator in October 1994, with 1 psu SSS difference over 8° of longitude. The tightness of this salinity front is certainly a common feature of the two OGCM simulations with interannual precipitation (Figures 7 and 8). In any case, looking at Figures 1, 7 and 8, it appears that the salinity front is very close to the trajectories and thus a good indicator of the oceanic zone of convergence.

As noted earlier, the salinity front is due to the convergence of the fresh water of the warm pool into the salty water of the cold tongue. Above these two oceanic regions, the respective areas of intense precipitation and evaporation follow the ENSO zonal displacements of the atmospheric convection [e.g., *Fu et al.,* 1986; *Delcroix,* 1998], and this could have been the reason for the displacement of the salinity front. However, several studies demonstrate that the salinity front is instead mainly driven by zonal advection. Using Geosat-derived surface currents, merchant ship SSS field, and outgoing longwave radiation derived precipitation, *Delcroix and Picaut* [1998] found that zonal advection appeared to be the main mechanism responsible for the displacement of the salinity front during the 1986-1989 El Niño-La Niña. With various data and, in particular, thermosalinograph onboard merchant ships over the 1992-95 period, *Hénin et al.* [1998] found that precipitation acts as a source of freshwater responsible for the existence of the salinity front, but the main mechanism responsible for the displacement of this front is zonal advection. *Cronin and McPhaden* [1998] have evaluated the upper ocean salinity balance in the western equatorial Pacific from data of the enhanced monitoring COARE array of moorings. They conclude that for timescales between a month and 2.5 years, SSS changes were weakly correlated with precipitation and were dominated by zonal advection. *Vialard and Delecluse* [1998b] developed a mixed layer budget method in order to compute the different terms acting on the temperature and salinity in the mixed layer of the OPA OGCM. They conclude that zonal advection is dominant in displacing the salinity front. Finally, the previous test with the GC model shows that the freshwater flux is not responsible for the zonal displacements of the salinity front. Large-scale surface currents in the vicinity of the equator are the dominant terms in driving the position of the front through zonal advection.

4.2. Eastern Edge of the Warm Pool and Salinity Front

One could wonder why there is a salinity front at the EWPCZ and not a temperature front. Whereas the net freshwater flux is of opposite sign in the warm pool and in the central equatorial Pacific, the surface net heat flux is positive all along the equator, with strong heating in the cold tongue slowly decreasing toward a weak positive heat flux in the warm pool [e.g., *Liu and Gautier,* 1990; *Liu et al.,* 1994]. East of the EWPCZ, cold SSTs result mainly from the equatorial upwelling, and their absolute values increase toward the west because of the less effective upwelling with the sloping thermocline along the equator. In addition, the equatorial upwelled water is mixed with the surrounding warmer water during its westward transport. Together with the atmospheric net heat flux, these result in a progressive SST warming toward the west. In any case the presence of a sharp SST front at the EWPCZ would have been hard to maintain because of the strong and relatively fast atmospheric response. On the contrary, SSS front cannot generate an atmospheric response. Therefore the salinity front delineates the separation between a SST gradient nearly null in the warm pool and a well-defined negative and nearly constant SST gradient farther east. This negative zonal SST gradient is part of the mechanisms that drives the westward surface winds [*Lindzen and Nigam,* 1987], and this separation is fundamental as the wind convergence and associated convection follow the zonal displacement of the EWPCZ.

When the movement of the warm and fresh pool is eastward, the zone of convergence is usually displaced in association with the eastern edge of the warm pool and the salinity front. The associated eastward displacement of the convective cells sustains the fresh water input into the ocean and helps maintaining the salinity front. During very strong El Niño, such as in 1982-1983, the zone of convergence eventually merges with the warm water of the far eastern equatorial Pacific and the fresh water extending off the Panama coast [*Delcroix et al.,* 1996]. In such extreme case the eastern edge of the warm pool and the salinity front are poorly defined and can extend east of the zone of convergence (Figure 1). Interestingly, the right panel of Figure 3 shows that during the 1997-1998 El Niño the warm pool advected by zonal currents is distinct (however, by <1°C) from the warm pool in the far east, induced, most probably, by the downwelling Kelvin waves and thus by the annihilation of vertical advection. Conversely, during La Niña when the movement of the warm pool is westward, the high-salinity cold water from the east penetrates into the warm pool. As shown in section 3, during some La Niña events the zone of convergence defined by the hypothetical drifter trajectory can pass the eastern edge of the warm pool together with its salinity front. In this extreme case, zonal advection is most probably overridden by the input of heat and freshwater flux from the atmosphere or other processes. The warm pool is seriously reduced in its zonal extent during a strong La Niña, but it never disappears [e.g., *Picaut and Delcroix,* 1995, Figure 2]. Hence apart from very strong El Niño and some La Niña events, the salinity front can be used to track the oceanic zone of convergence.

The delineation of the eastern edge of the warm pool

is not as straightforward. As noted above, it corresponds to the separation between a SST gradient nearly null in the warm pool and a negative SST gradient farther east. Together with the insufficient number of in situ measurements and the deficiency of satellite measurements in cloud-covered regions, one cannot expect a perfect determination of the eastern edge of the warm pool. The 29°C isotherm was chosen as the highest nearly uninterrupted integer isotherm (Figure 1), but observations (Figures 2-5) and model simulations (Figures 7-8) suggest that an isotherm a little inside the warm pool (29.1° or 29.2°C) could have been more appropriate if less discontinuous. The use of hypothetical drifter to infer the position of the oceanic zone of convergence has some flaws (see section 4.3). Even if SST and SSS on the eastern edge of the warm pool are mainly driven by zonal advection, many other mechanisms influence their behavior (e.g., vertical and meridional advection, heat, and freshwater fluxes). In conclusion, it should not be a surprise if the hypothetical drifter trajectories, 29°C, and salinity front are not strictly collocated.

4.3. Current Convergence and Equatorial Trapping

The convergence of the EWPCZ is due to the mean zonal currents in the equatorial band that are weakly eastward in the warm pool and clearly westward in the cold tongue (Figures 10 and 11, upper panels). However, the extensive zonal displacements of the eastern edge of the warm pool associated with ENSO (Figure 1) is due to the changes in strength of the zonal currents

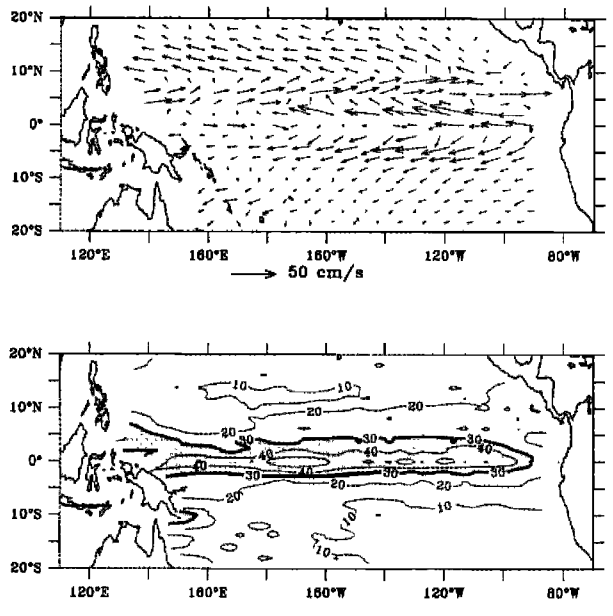

Figure 10. Near-surface currents over the tropical Pacific derived from the drifting buoy climatology: (upper panel) mean current vectors and (lower panel) standard deviation of zonal currents. Shaded area corresponds to values >30 cm s^{-1}.

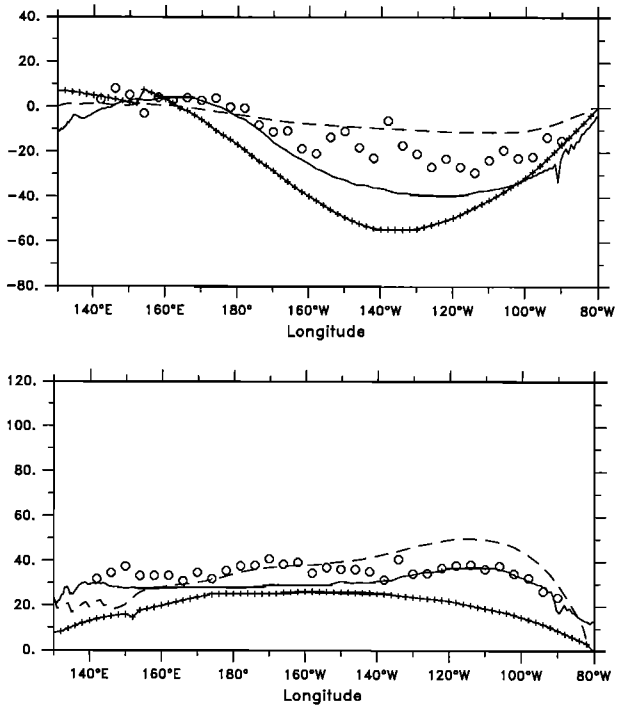

Figure 11. (upper panel) Mean zonal surface currents and (lower panel) their standard deviations, along the equator and averaged within 4°N-4°S, from the drifting buoy climatology (open circle), linear model (pluses), OPA model (solid line) and GC model (dashed line). Units are cm s^{-1}.

along the equatorial band (Figures 10 and 11, lower panels). Westward shifts of the EWPCZ are associated with a stronger than normal SEC over the cold tongue during La Niña [*Frankignoul et al.*, 1996], and eastward shifts are mostly due to eastward jets. These jets are usually driven by westerly wind bursts [*McPhaden et al.*, 1992; *Delcroix et al.*, 1993], but freshwater-driven salinity gradient is another potential driving force [*Roemmich et al.*, 1992]. Most of all, displacements of the EWPCZ is due to the fact that these varying surface zonal currents are quite often toward the same direction during a number of months, as seen, for example, on Figure 3. The convergence of the mean zonal currents is not well defined in the equatorial band (Figures 10 and 11, upper panels), unlike the variations of these currents that are clearly trapped to the equator (Figure 10, lower panel). Equatorial wave dynamics are responsible for this trapping of the zonal currents, as already noted in observations by *Delcroix et al.* [1994] and *Boulanger and Menkes* [1995]. Like the zonal currents, the salinity changes associated with the displacement of the EWPCZ are trapped to the equator. Figure 12, taken with Conductivity-Temperature-Depth (CTD) and current measurements from 42 cruises along 165°E, suggests a trapping scale of about 4° [*Delcroix and Picaut*, 1998], which can be dramatically evidenced by continuous cross-equatorial SSS measurements [*Hénin et al.*, 1998, Figure 8].

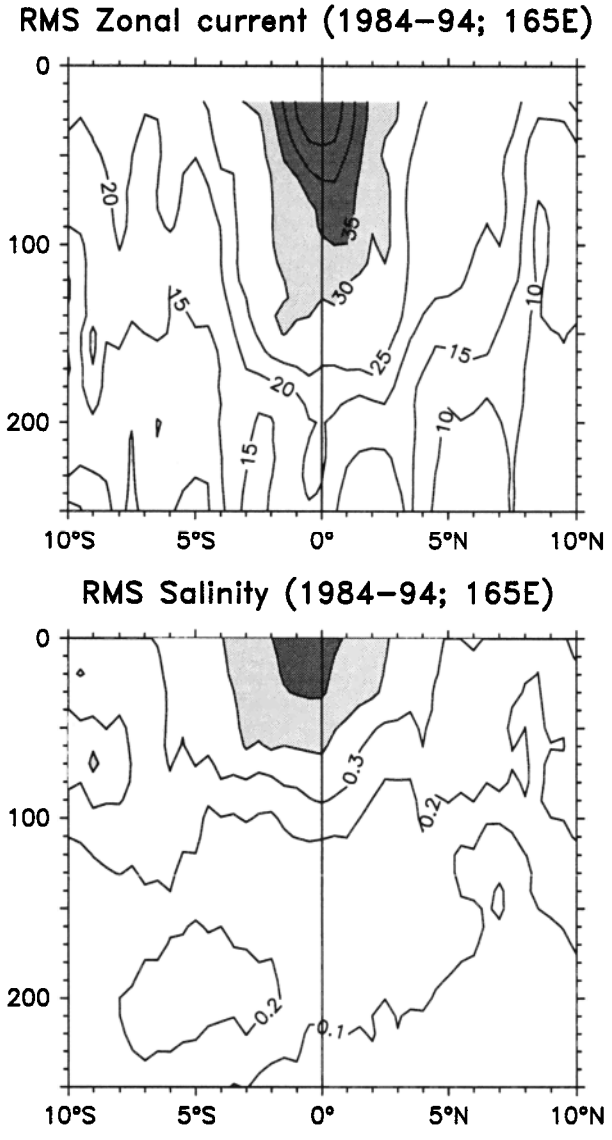

Figure 12. Standard deviations of (upper panel) the zonal currents and (lower panel) salinity, from 42 cruises along 165°E. Contours are 5 cm s^{-1} and 0.1 psu respectively.

A better estimation of this trapping is necessary in order to determine the width of the equatorial band affected by the displacement of the oceanic zone of one-dimensional convergence. Additional calculations were done with the observed and simulated current fields using hypothetical drifters with different drogue sizes (from 1°N-1°S to 6°N-6°S). The displacements of the drifters were compared to the displacements of the 29°C isotherm and of the salinity front averaged in the same equatorial band. The mean ratio of the standard deviations of these displacements (around 16° of longitude) is 1.15 for 1°N-1°S, 1.06 for 2°N-2°S, 0.98 for 4°N-4°S, and 0.88 for 6°N-6°S. The relative difference between 1°N-1°S and 6°N-6°S is partly due to the presence of eastward surface jets in the warm pool that are really trapped to the equator [e.g., *McPhaden et al.,* 1992; *Ralph et al.,* 1997], in contrast to the SEC in the east, which is broader, as seen in the upper panel of Figure 10 and discussed by *Philander and Pacanoswki* [1980]. Overall, the zone of convergence defined by hypothetical drifter trajectory is most often associated with the salinity front centered around 34.8 psu and the 29°C isotherm in a latitudinal range of 2°-5° around the equator, which is of the same order of magnitude as the equatorial radius of deformation.

Whereas interannual variations of current and salinity are very much trapped to the equator, the displacements of the eastern edge of the warm pool occurs over a wider meridional range. Once the EWPCZ starts to be displaced along the equator by the variations of zonal current within about 4°N-4°S, the seasonal heating intervenes. Together with diffusion and meridional advection, this results in the zonal migration of the eastern edge of the warm pool over a broader area. In particular, the zonal displacement is slowly shifted on one side of the equator by as much as 10° of latitude because of the seasonal heating. Such features were particularly discernible during the strong El Niño events of 1982-1983 and 1997-1998. Similar patterns, but in the other direction, are also evident during the demise of El Niño and its shift into La Niña. The combination of the notable zonal displacements by equatorial currents and of the small meridional migration by seasonal heating explains the elliptic nature of the centroid of the warm pool as evidenced by *Yan et al.* [1997]. However, the fundamental mechanism for moving the eastern edge of the warm pool eastward or westward during ENSO events remains zonal advection, which acts basically around the 4°N-4°S equatorial band.

4.4. Hypothetical and Real Drifters, Continuous Zonal Transport

A comparison between real and hypothetical drifter behaviors is now presented. This will fully justify the use of a hypothetical drifter as a tracer for water mass convergence in the equatorial band and the inherent omission of the meridional component of the currents. In the warm pool, eastward displacements under a series of westerly wind bursts are mostly associated with equatorial convergence. As a consequence, particles of water usually stay for several months in the equatorial band while traveling toward the central equatorial region, as shown from drifter observations by *McPhaden et al.* [1992] and *Ralph et al.* [1997]. Simulations of "real" drifter trajectories in the OPA model suggest that a significant part of the drifters launched in the warm pool reached the EWPCZ defined by the salinity front (Figure 13). On the other hand, real drifters launched in the eastern equatorial region, moved westward by the trade wind-induced SEC, are subject to equatorial divergence. This divergence results, on average, in a 5 cm s^{-1} meridional current [*Poulain,* 1993], and a single drifter launched near the equator will leave the 4°N-

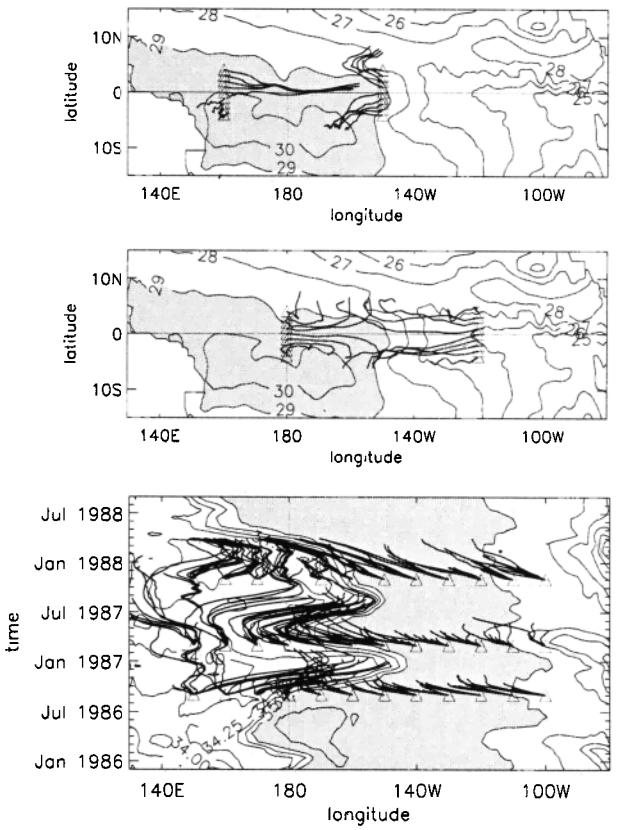

Figure 13. Trajectories of real drifters launched in the OPA surface currents: (upper panel) 3 month trajectories starting from 160°E on September 1, 1986, and 5 month trajectories starting from 150°W on September 1, 1986; (middle panel) 3 month trajectories starting from 180° on November 1, 1986, and 5 month trajectories starting from 120°W on July 1, 1986; (lower panel) trajectories starting on September 1986, March 1987, and November 1987 along the equator plotted as long as they stay in the 4°N-4°S equatorial band and over the time-longitude distribution of the simulated SSS (contour every 0.25 psu; values >35 psu darkly shaded). The background in the upper and middle panels is the December 1986 simulated SST (contour every 1°C; values >29°C darkly shaded).

4°S equatorial band in about 3 months while traveling, on average, 3000 km westward [*Hansen and Swenson,* 1996]. Even if surface water parcels seldom reach the eastern edge of the warm pool, there is a continuous westward transport of mass toward this region [*Wyrtki,* 1985]. This is illustrated on Figure 13 with a series of real drifters launched successively into the SEC simulated by the OPA model, which ultimately converge toward the EWPCZ defined by the salinity front.

Such continuous westward transport is also evidenced through the existence of a permanent downward slope in sea surface height along the equator in the eastern-central Pacific. In fact, with the existence of a small upward slope of the sea surface in the warm pool [*Wyrtki,* 1984; *McPhaden et al.,* 1998] the EWPCZ inferred from hypothetical drifters corresponds approximately to the convergence of water masses as indicated by the intersection of the westward and eastward slopes. Dynamic height anomaly measurements along the equator are too scarce to evidence such sea level convergence and its zonal displacement [e.g., *Mangum et al.,* 1990; *Kuroda and McPhaden,* 1993]. Hence surface dynamic heights simulated from the OPA model are used to detect this feature. As shown on Figure 14, the absolute maximum of surface dynamic height, which approximates the encounter of the eastward and westward sea level slopes, has a tendency to follow the displacement of the hypothetical drifter and of the eastern edge of the warm pool. Precipitation, through its effect of salinity, can account for up to 30% of the sea level signal over the warm pool [*Chambers et al.,* 1998; *Maes et al.,* 2000], and thus may explain some of the discrepancies, such as in 1992. Furthermore, a lag between the adjustment of dynamic heights and currents is expected, especially in the Ekman layer. As indicated by various maps of sur-

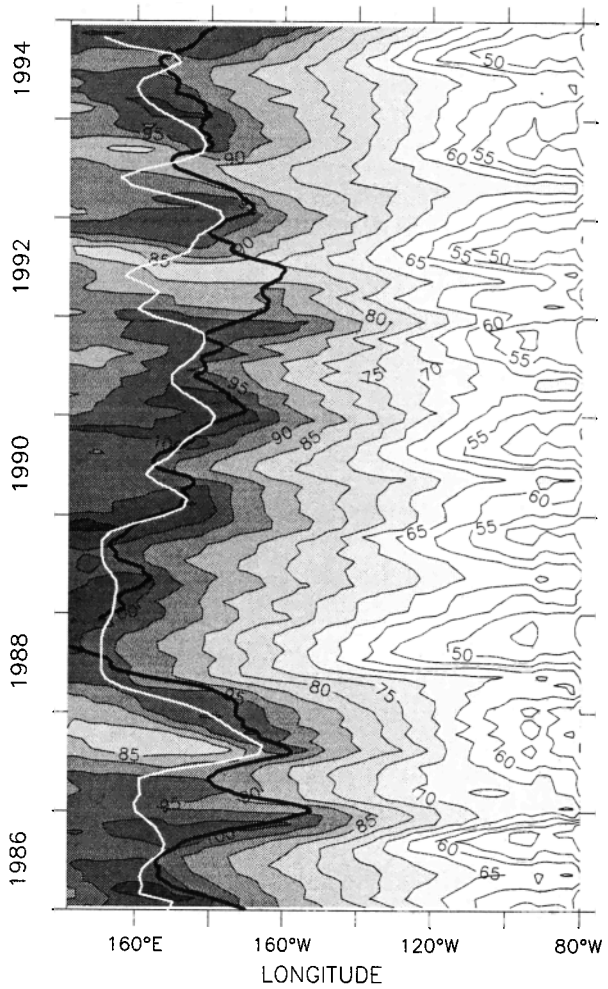

Figure 14. Longitude-time distribution of 4°N-4°S averaged surface dynamic height relative to 200 dbar calculated from the OPA model. The white line corresponds to the absolute maximum of surface dynamic height, and the dark line corresponds to the zone of convergence defined by hypothetical drifter trajectories (as in Figure 7).

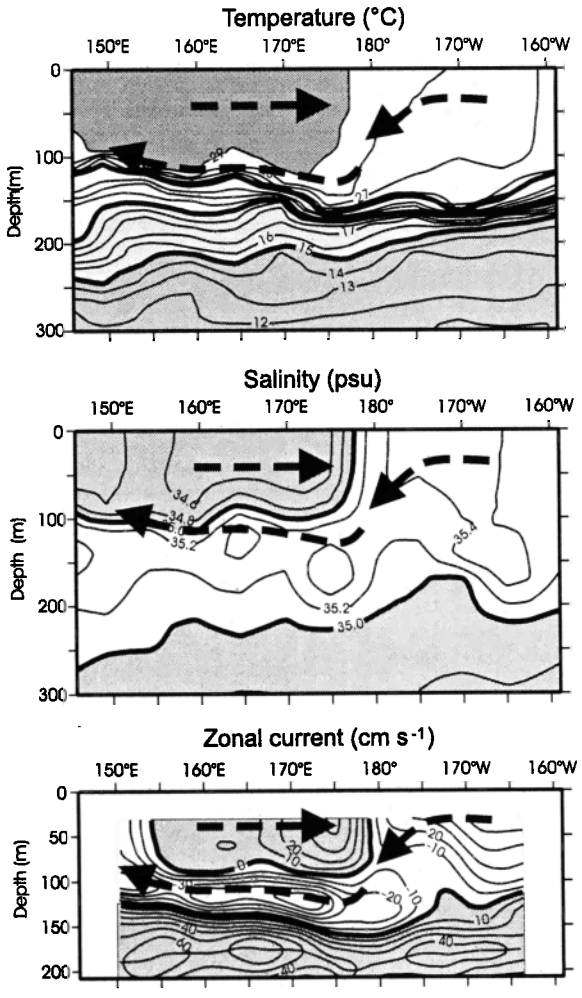

Figure 15. Zone of convergence and barrier layer illustrated from an observed section along the equator of (upper panel) temperature, (middle panel) salinity, and (lower panel) zonal currents. The arrows follow the maximum of currents and depict the surface convergence, the subduction and the formation of the barrier layer (adapted from *Kuroda and McPhaden* [1993]).

face dynamic heights relative to different reference levels (not shown), much of this surface dynamic heights encounter is explained by the variation of dynamic heights above 100 m.

4.5. Barrier Layer

According to *Vialard and Delecluse* [1998b], the convergence of the SEC (flowing from the surface down to 70 m) and the eastward jets (flowing only in the upper 30-40 m) results in a subduction of the salty and dense water brought by the SEC under the fresh and light water of the warm pool. This yields to the formation of the barrier layer, which also follows the zonal displacements of the warm pool [*Ando and McPhaden,* 1997]. These important features are illustrated on Figure 15 through the synoptic measurements of CTD and currents taken along the equator in January-February 1990 [*Kuroda and McPhaden,* 1993]. The lower and middle panels of Figure 15 show the convergence of surface zonal currents into the salinity front and suggest the subduction pathway of the cold and high-salinity water of the cold tongue under the warm and fresh pool. The upper panel of Figure 15 indicates that this high-salinity water subducts just above the thermocline, resulting in the so-called barrier layer. Note that the barrier layer can be formed south of the equator through a related process [*Shinoda and Lukas,* 1995; *Vialard and Delecluse,* 1998b] and inside the warm pool by direct rainfall [*You,* 1995] and, consequently, subsists over most of this region [*Sprintall and Tomczak,* 1992]. Because of the barrier layer, the wind forcing is particularly effective over the warm pool as the momentum is trapped in the upper layer [*Vialard and Delecluse,* 1998b]. In addition, the warm pool beeing composed of low-density fresh and warm water can slide easily over the high-density cold and salt water of subtropical origin. The barrier layer thus contributes to the movements of the EWPCZ. The barrier layer also isolates the warm pool from below, as it obstructs entrainment of the colder water into the surface layer [*Lukas and Lindström,* 1991; *Vialard and Delecluse,* 1998b]. In a similar way, the zonal salinity front and the subsequent density front may limit the exchange between the warm pool and the equatorial region farther east. The existence of these vertical and zonal "barriers"could, in addition to air-sea flux control [e.g., *Wallace,* 1992], explain why SSTs over the warm pool are relatively constant and high.

5. Consequences for ENSO and Biogeochemical Phenomena

Important consequences of the EWPCZ and its displacements have already been discussed, including the formation of the barrier layer. This sections briefly discusses other consequences for ENSO and biogeochemical phenomena.

5.1. ENSO Coupling in the Central-Western Equatorial Pacific

The advance and retreat, in phase with ENSO, of the eastern edge of the warm pool over the central equatorial Pacific induce SST changes in the 26°-29°C range (Figure 1). Within this range, SST provides enough moist static energy for ascending air and creates deep atmospheric convection [*Betts and Ridgway,* 1989]. At the air-sea interface this results into a convergence of winds over the warm waters [*Deser and Wallace,* 1990; *Clarke,* 1994]. *Lindzen and Nigam* [1987] proposed another mechanism for driving the surface wind convergence through the atmospheric pressure anomalies induced by the SST gradient between the warm pool and the cold tongue. These two mechanisms are, in fact, closely related [*Wu et al.,* 1999], and warm waters within the range 26-29°C are still indispensable for

building up surface wind convergence and deep atmospheric convection. This explains why surface winds and rainfall closely follow the movement of the eastern edge of the warm pool, as shown on Figure 1 of this study and on Figure 6 by *Delcroix* [1998]. Farther east, the ocean has generally a greater ENSO signature in terms of SST anomaly, but except during very strong El Niño, its absolute SST is not high enough to induce significant atmospheric convection and surface wind convergence (compare on Figure 1 the displacements of the -20 m^2 s^{-2} contours of zonal wind stress in the east and west). Hence the zonal displacement of the EWPCZ is fundamental for establishing the ENSO coupled system in the central-western equatorial Pacific. Besides, the character of the coupled system in the central equatorial Pacific is undeniable as it is impossible to sort out cause and effect: the EWPCZ is displaced by the winds and surface currents, but the winds are changed by the displacements of the EWPCZ. The eastward displacement of the EWPCZ during El Niño increases the fetch of the westerly winds over the warm water [*Kessler et al.,* 1995] through their penetration into the central equatorial Pacific. Conversely, the westward displacement of the EWPCZ during La Niña reduces the fetch of the westerly winds and results in the penetration of the easterly winds into the western equatorial Pacific (Figure 1).

Several studies highlighted the key role of the interannual variations of SST in the central equatorial Pacific (and thus of the EWPCZ) in setting up global atmospheric teleconnections [*Barnston et al.,* 1997]. *Graham et al.* [1994] found a link between the Northern Hemisphere winter atmospheric circulation and the equatorial Pacific SST anomalies within 160°E and 140°W, the region affected by the displacement of the EWPCZ. This is in agreement with the studies of *Palmer and Mansfield* [1984] and *Geisler et al.* [1985], who found that the western and central equatorial Pacific SST is more effective than the eastern equatorial Pacific SST for exciting midlatitude responses, such as the Pacific North American (PNA) pattern. With its displacement eastward during El Niño and westward during La Niña the EWPCZ induces SST changes around the 28°C threshold required for organized convection in separate equatorial regions. According to *Hoerling et al.* [1997], this geographical distinction induces teleconnection responses over the PNA region shifted by at least 15° and thus may explain part of the nonlinearity of the ENSO teleconnection between El Niño and La Niña.

5.2. A Revised Theory of the Delayed Action Oscillator of ENSO

The SST-winds-ENSO interaction is mainly located in the central-western equatorial Pacific. Yet, the intermediate coupled models, which led to the discovery of the delayed action theory of ENSO, had their strongest coupling over the central-eastern side of the basin [*Zebiak and Cane,* 1987; *Battisti,* 1988; *Schopf and Suarez,* 1988]. As an example, the Zebiak and Cane model simulates the ENSO air-sea interaction in a region as much as 30° of longitude east of the observed one [*Mantua and Battisti,* 1994]. A reason is the excessive weight given to the vertical displacement of the thermocline for reproducing SST variations in the eastern equatorial basin (i.e., NINO3). In any case this theory is fascinating as it provides a rather simple explanation for the demise of El Niño and its shift into La Niña. It is the successive arrival of upwelling equatorial Kelvin waves, resulting from the reflection of upwelling equatorial Rossby waves on the western ocean boundary, that acts to damp the growing SST-wind coupling of the equatorial Pacific by raising the thermocline. The recent results of *Boulanger and Menkes* [1999] indicate that the western boundary is a good reflector of equatorial Rossby waves. However, there are still observational doubts concerning the importance of the western boundary reflection versus local wind forcing in view of the delayed action oscillator scenario [*Delcroix et al.,* 1994; *Boulanger and Menkes,* 1995; *Boulanger and Fu,* 1996; *McPhaden and Yu,* 1999; *Delcroix et al.,* 2000]. The eastern boundary also seems to be a rather good reflector of equatorial Kelvin waves into equatorial Rossby waves [*Boulanger and Fu,* 1996; *Boulanger and Menkes,* 1999]. *Picaut and Delcroix* [1995], together with *Delcroix et al.* [2000], found out that during El Niño, interannual Rossby waves issued from the eastern boundary can help push back the EWPCZ and hence participate in the shift from El Niño to La Niña (Figure 3).

On the basis of the insufficiencies of the delayed action oscillator theory of ENSO, the discovery of the EWPCZ, and the impacts of reflected equatorial waves on its zonal displacements, *Picaut et al.* [1997] proposed a revision of the delayed action oscillator theory in which zonal advection of the eastern edge of the warm pool, mean converging zonal currents, and reflection of equatorial waves on both ocean boundaries are fundamental to the oscillatory nature of ENSO. The simple coupled model, used to illustrate this revised theory, resulted in an ENSO coupled system in the right place, namely, in the central-western equatorial Pacific. As stated by *Picaut et al.* [1997], the model used was oversimplified and was not intended to explain the complete scenario of the ENSO oscillation. In particular, being limited to zonal advection, during a strong El Niño when warm SSTs are uniformly spread into the east, the modeled return (westward) flow cannot bring cold water in the central equatorial Pacific to develop a La Niña (Figure 3). Hence a source of cold water is needed in the east that can be provided by the uplifting of the thermocline. This can be done through the readjustment of mass along the equator with the returning flow, the equatorial divergence associated with this westward flow, or the arrival of upwelling Kelvin waves, following the original delayed action oscillator theory. Furthermore, without any leak of energy in the deep ocean [*McCreary,*

1984; *Dewitte et al.,* 1999] the relative contribution of reflected equatorial waves on the two ocean boundaries in the ENSO oscillation cannot be precisely determined by the simple model. In any case the basic oscillation of ENSO intrinsic to the equatorial Pacific basin is most likely a combination of the original delayed action oscillator theory and the revised one, with horizontal and vertical advection acting together.

5.3. Transfer of Mass and Heat and ENSO Memory

It is important to realize that the EWPCZ and its displacements along the equatorial band are not limited to the surface. Hence the associated transports of mass and heat can be considerable and need to be investigated as they are the grounds of the "memory"of the ENSO system. Following the pioneer's work of *Wyrtki* [1975, 1985] on the transport of mass associated with the eastward displacement of the warm pool during El Niño, *McPhaden and Picaut* [1990] calculated the variation of zonal transport between the 1986-1987 El Niño and the 1988-1989 La Niña from in situ current observations. They found a change in the equatorial band as large as 58 Sv. This was comparable to the estimate of *Delcroix et al.* [1992] over the same period. Figure 12, which illustrates the equatorial trapping of the near-surface salinity and currents associated with the EWPCZ, indicates that the trapping of current and salinity extends down to 50-100 m. There are not enough observations of currents in the vertical to find out the maximum depth of the zone of convergence, but profiles of salinity measured along the equator [*Kuroda and McPhaden,* 1993; *Eldin et al.,* 1997] suggest it to be around 40-60 m. Additional tests with hypothetical drifters launched at various depths in the OPA model confirm such depths [see also *Vialard and Delecluse,* 1998b]. A calculation based on Figure 12 gives 18 Sv for the standard deviation of the zonal transport in the first 50 m and within the 4°N-4°S band. Thirty six (18 × 2) Sv is nearly half the change of the previous instantaneous estimates of zonal transport over the first 100 m during the well-defined 1986-1989 El Niño-La Niña cycle. These huge transfers of mass and heat along the equatorial band lead to anomalous accumulation or depletion of mass on both sides of the equatorial basin. As inferred from Figure 14, this results in an ENSO anomalous seesaw-like pattern in sea level and thermocline depth along the equator [e.g., *Wyrtki,* 1985; *Delcroix,* 1998].

In fact, it is the repeated occurrences of downwelling Rossby waves, excited by the dominant easterly trades in the central-eastern Pacific, that feed the reservoir of mass and heat in the warm pool. Because of the slow propagation of the Rossby waves, the reservoir of heat is not in equilibrium with the winds, and consequently, it is the most important memory of the ENSO system [*Battisti and Hirst,* 1989; *Schneider et al.,* 1995]. Through short Rossby waves along the western boundary and then equatorial Kelvin waves the mass and heat of this nonadjusted reservoir are transferred along the equator and into the eastern boundary [*Neelin et al.,* 1998]. So, one has to consider more the effect of the slow transfer of mass and heat accompanying the displacement of the EWPCZ along the equator than the rapid propagation of Kelvin waves and its effect on the eastern equatorial thermocline.

5.4. Exchange of CO_2 With the Atmosphere and Biological Production

The equatorial Pacific Ocean is known to be the largest natural source of CO_2 into the atmosphere [e.g., *Feely et al.,* 1999]. It is also a potential source of new production in the ocean through the import of nutrients to the euphotic zone [*Chavez and Barber,* 1987]. The cold tongue and the warm pool have different biogeochemical structures. The warm pool is nearly oligotrophic and characterized by a nutrient-depleted surface layer above a deep thermocline and a nutrient-rich deep layer. Its air-sea interface is also specific with partial pressures of CO_2 (pCO_2) close to equilibrium. The cold tongue is eutrophic, with the equatorial upwelling bringing nutrients and inorganic carbon to the surface. Hence, the sea surface always has high pCO_2, and the cold tongue is the major source of CO_2 to the atmosphere.

The discovery of the EWPCZ, as a clear separation between the cold tongue and the warm pool and its ENSO displacements [*Picaut et al.,* 1996], led to some questioning in the biogeochemical community. Knowing that SSTs over the cold tongue exhibit a regular increase from the far eastern equatorial Pacific to the warm pool, a rapid modification of several of the biogeochemical parameters was not anticipated in the vicinity of the EWPCZ. From the results of several cruises, *Inoue et al.* [1996] noted several sharp changes in the longitudinal distribution of pCO_2 along the Pacific equator and their association with rapid SSS changes. *Inoue et al.* [1996] established a relationship between the location of the pCO_2 changes and the SOI but they were short of explanation. As illustrated in Figure 9, the changes of sea surface concentration of CO_2 and SSS are associated with the EWPCZ that separates the warm pool from the cold tongue. Through a compilation of numerous pCO_2 data, *Boutin et al.* [1999] determined a relation between pCO_2 and satellite SST and wind speed. They found that the total change of CO_2 flux over the equatorial Pacific could vary by a factor of 5 from the 1986-1987 El Niño to the 1988-1989 La Niña. They attribute a significant portion of this change to the displacements of the EWPCZ that make the surface area of the outgassing cold tongue quite variable.

Some other biogeochemical parameters may change rapidly around the EWPCZ. From the results of the Flupac cruise along the equator in September-October 1994 [*Le Borgne et al.,* 1995] it was noted that there was a sharp increase of zooplancton biomass between

172° and 174°W [*Le Borgne and Rodier,* 1997] associated with the salinity front (Figure 9) and hence with the EWPCZ. However, because of diffusion, consumption, and high-frequency physical forcing [*Eldin et al.,* 1997], the increase of nitrate, phosphate, and silicate occurred a little farther east. With very few synoptic biological measurements along the equator one has to rely on coupled models in order to perceive the behavior of the complex biophysical interaction. This was done by *Stoens et al.* [1999] through the addition of a nitrate transport model with a simple biological sink into the OPA OGCM over the 1992-1995 period. The coupled model was favorably compared to the Flupac observations, and a sharp front of new production was found, over the complete 1992-1995 period, coincident with the salinity front depicted in Figure 7. Hence the ENSO displacements of the EWPCZ appear to alter considerably the new production of the Pacific. However, one cannot claim that the EWPCZ is a clear separation between oligotrophic and eutrophic waters. The oligotrophic characteristics of the warm pool is far from being permanent, as noted by in situ pulses of phytoplancton growth by *Dandonneau et al.* [1988] and more recently by the Sea-viewing Wide Field-of-view Sensor (SeaWiFS) satellite [e.g., *Murtugudde et al.,* 1999]. Detailed analyses of the SeaWiFS data and biogeochemical in situ data, in parallel with physical-biological coupled model experiments, will clarify the relation between the formation and evolution of the EWPCZ and its impacts on the biogeochemistry of the Pacific Ocean.

5.5. Displacement of Tuna Fishery

In the 1960-1970s, nearly all of the U.S. purse seine tuna fleets were situated in the eastern tropical Pacific. In addition to economical reasons, the poor fishing conditions in the eastern Pacific during the 1982-1983 El Niño has stimulated many U.S. purse seine vessels to move west, where a Japanese fleet had already been active for a few years [*Fonteneau,* 1997; *Doulman,* 1987]. In fact, the warm pool was found to be much more productive than expected, and currently, it represents the most important stock of tunas in the world, with about 1.5 million tons caught each year (mostly skipjack tuna), as compared to the world harvest of 3.5 million tons (all tuna species). Interestingly, this annual catch in the warm pool, worth about 1.7 billion of Euros, is carried out by about 1300 tuna boats fishing mostly in the exclusive economic zones of the western Pacific Islands.

Convergence zones are known to aggregate plankton and micronekton and hence large predators [e.g., *Yoder et al.,* 1994]. With the discovery of the EWPCZ a group of scientists looked for a possible relation between the movement of the tuna fishery and ENSO [*Lehodey et al.,* 1997]. *Lehodey et al.* [1997] used catch per unit effort (CPUE) to determine the relative abundance of fish stock. To avoid biases in this abundance index, only the skipjack data of the U.S. purse-seine fleet were analyzed over the 1988-1995 period (extended later to 1998). During the 1988-1989 La Niña, the catches of the purse seine fleet were concentrated in the reduced warm pool west of 160°E. In contrast, during the series of three weak El Niño events over the 1991-1995 period, skipjack tunas were caught in an area extending eastward with the warm pool. The relation with the displacement of the EWPCZ and hence the phases of ENSO was corroborated by a correlation analysis between the longitudinal center of gravity of CPUE and the eastern edge of the warm pool. A correlation coefficient of 0.75 with zero lag and a ratio of 0.8 for the standard deviations were found between the monthly time series of longitudinal center of gravity of CPUE and the 29°C isotherm [*Lehodey et al.,* 1997]. Interestingly, most of the skipjack tuna catch occurs within 5°N-5°S, supporting the probable role of the equatorially trapped dynamics of the EWPCZ in the mechanism leading to surface tuna movement and aggregation.

Knowing that skipjack tunas are opportunistic feeders and require a large amount of food (possibly 10-15% of their own weight per day), it was a surprise to find such concentration of tunas in the oligotrophic water of the warm pool. The existence of the EWPCZ is likely the reason for these concentrations of food and tunas and their zonal displacement. Without direct means to measure and quantify the tuna diet (ranging from large zooplancton to anchovy) on the scale of the warm pool, one has to rely on model simulations in order to apprehend tuna forage. This was tentatively done by *Lehodey et al.* [1998] through a simple food web transfer of new production to tuna forage. The new production was obtained from the coupled model of *Stoens et al.* [1999], briefly discussed in section 5.4, and the transfer was parameterized according to the food chain length and redistributed by the horizontal currents derived from the OGCM. Encouraging results support the idea that the mechanism of the formation of the EWPCZ (i.e, the convergence in time and space of the infrequent eastward flow in the west and the more permanent westward flow in the east) is also at work in the aggregation of the animals that represent the net production of the equatorial upwelling.

6. Conclusions

The existence of an oceanic zone of confluence, or one-dimensional convergence on the eastern edge of the warm pool, has been demonstrated in several studies through the examination of several independent observational and numerical model data sets. Here we have synthesized and completed these results with additional analyses to show that this zone of convergence (EWPCZ) clearly separates the warm pool of the western equatorial Pacific from the cold tongue in the east. Because of the very different near-surface salinity of these two regions, this zone of convergence is generally seen as a well-defined zonal salinity front. Most importantly, the alternate and opposite variations of the near-

surface zonal currents in both regions during a number of months result in the displacements of the EWPCZ. This happens within the equatorial band and over thousands of kilometers, eastward during El Niño and westward during La Niña. Such displacements, in synchrony with the Southern Oscillation, are an essential feature of the ENSO coupled system in the central equatorial Pacific. Once the EWPCZ starts moving eastward (e.g., under a series of westerly wind bursts), the eastern edge of the warm pool expands and so does the fetch of the westerly winds. Hence the system goes into an El Niño growing mode. Conversely, when the easterlies in the central equatorial Pacific strengthen, the warm pool is pushed westward. This reduces the fetch of the westerly winds and thus increases La Niña and the retreat of the warm pool.

These findings were made possible through the use of numerous in situ and satellite data and the output of three classes of ocean model. A Lagrangian approach, through the use of hypothetical drifters with a drogue covering the equatorial band, appeared to be best suited for integrating in space and time the strength and duration of the near-surface zonal current. Hence zonal advection appears to be dominant for changing SST and SSS in the central equatorial Pacific. ENSO can therefore be characterized by two modes: one in the central equatorial Pacific dominated by zonal advection and local wind forcing and, the other in the eastern equatorial Pacific dominated by vertical advection through remotely forced Kelvin waves. The main difference between these two modes is their ability to be locally sustained. The first one concerns absolute SST around the 28°C threshold required for organized atmospheric convection and appears to be essential to developing and maintaining the ENSO coupled system. The second concerns absolute temperature generally lower than this threshold, and except during very strong El Niño, it needs to interfere with the central and western equatorial regions to sustain the ENSO coupled system. As suggested by *Barnston et al.* [1997], future ENSO studies should focus more on the absolute SST in the NINO3.4 region (150°W-160°E, 5°N-5°S), and not so much on the anomalous SST in the NINO3 region (90°-150°W, 5°N-5°S).

A revision of the delayed action oscillator theory was thus proposed in which the EWPCZ, zonal advection, mean converging zonal currents, and equatorial waves are fundamental to the ENSO oscillation [*Picaut et al.*, 1997]. In this concept the basic period of ENSO corresponds to the time it takes for the EWPCZ to be moved by near-surface zonal currents, from eastward to westward (and vice versa). The scrutiny of the EWPCZ and its displacements may bring less uncertainty on the phase locking of ENSO with the seasonal cycle. La Niña can be seen as a penetration of the seasonal upwelling of the cold tongue into the warm pool. Conversely, El Niño can be seen as a penetration into the cold tongue of the eastern edge of the warm pool, which is nearly unaffected by the seasonal cycle [Figure 1 and *Picaut and Delcroix,* 1995]. This may be an explanation of the fact that La Niña is more phase-locked to the seasonal cycle than El Niño (J. Shukla, personal communication, 1998). In any case, coupled ENSO prediction models must be able to reproduce correctly the EWPCZ and its displacements at the right location. For example, the use of linear ocean models in the 1980s forced more weight to be put into the vertical displacements of the thermocline over the cold tongue. This can now be explained by the simulated EWPCZs, which were too far into the warm pool (Figure 6), and thus could not affect the SST much by moving near-isothermal waters. As a result, the simulated ENSO coupled systems were too far into the eastern part of the basin compared to observations [*Mantua and Battisti,* 1994; *Hirst,* 1988; *Battisti and Sarachik,* 1995].

The zonal displacement of the EWPCZ does not concern the surface layer only. Observations and model studies indicate that this phenomenon affects the first 40-60 m and covers the equatorial band within about 4°N-4°S. This implies tremendous redistribution of mass and heat within the equatorial wave guide (approaching the total transport of the Kuroshio) and, consequently, in the meridional direction. This deserves further attention, especially knowing that these transfers of heat are essential to the ENSO memory. In addition, more needs to be done for a better understanding of the relation between the EWPCZ and the barrier layer. TOGA-COARE [*Webster and Lukas,* 1992; *Godfrey et al.,* 1998] continues to bring valuable information on the behavior of the ocean-atmosphere system near the center of the warm pool. However, a smaller dedicated experiment on the eastern edge of the warm pool, combining ocean-atmosphere field experiment and modeling study, should certainly improve the understanding of the EWPCZ in relation to the physics of the ENSO coupled system.

Several studies have already looked at the physics of the eastern edge of the warm pool [*Picaut et al.,* 1997; *Vialard and Delecluse,* 1998b; *Clarke et al.,* 2000], but the evidence of the EWPCZ has also attracted several scientists of the biogeochemistry community. The discovery of the ENSO displacements of the world's most important tuna fishery, most likely in association with the EWPCZ [*Lehodey et al.,* 1997], has a great potential for improving commercial fishing and its management. However, more observations and physical-biological models are needed to determine the explicit role of the EWPCZ in the concentration of tunas in an oligotrophic region. The outgassing of CO_2 into the atmosphere within the equatorial Pacific is dependent on the location of the EWPCZ [*Boutin et al.,* 1999]. In particular, there is a substantial reduction of the surface of outgassing and consequently of release of CO_2 during the El Niño eastward displacement of the warm pool. This may compensate a little the long-term increase of the extent of the warm pool (Figure 6) if this

extent is related to global warming rather than to long-term natural climate variability. In any case the three components of the 15 year long Climate Variability and predictability (CLIVAR) program will certainly answer some of the questions related to the EWPCZ.

Acknowledgments. The authors are very grateful to a number of persons who provided different types of data: Mike McPhaden and Paul Freitag for the moored TAO currents; Gilles Reverdin, Claude Frankignoul, and Fabrice Bonjean for their bimonthly surface current field; Sharon Lukas and Peter Niiler for the climatology of surface current; Dick Reynolds for the NCEP SST; David Legler and Jim O'Brien for their FSU wind stress; and the CLS/AVISO group for the TOPEX/Poseidon sea level product. Comments on the manuscript by Allan Clarke, Christophe Maes, Mike McPhaden, and especially, the two anonymous reviewers are greatly appreciated. We thank Jim Christian, Mark Verschell, and Patrick Lehodey for their comments on the biogeochemical section and Bernard Brunet, Alain Poisson Bernard Schauer, and Robert Le Borgne for their authorization to reproduce Figure 9. Most of the writing by the first author was done during his 2 year visit at NASA Goddard Space Flight Center. This work was supported by IRD, PNEDC, CNES, and NASA (grant 621-55-04).

References

Ando, K., and M. J. McPhaden, Variability of surface layer hydrography in the tropical Pacific Ocean, *J. Geophys. Res., 102,* 23,063-23,078, 1997.

Barnston, A. G., M. Chelliah, and S. B. Goldenberg, Documentation of a high ENSO-related SST region in the equatorial Pacific, *Atmos. Ocean, 35,* 367-383, 1997.

Battisti, D. S., Dynamics and thermodynamics of a warming event in a coupled tropical atmosphere-ocean model, *J. Atmos. Sc., 45,* 2889-2919, 1988.

Battisti, D. S., and A. C. Hirst, Interannual variability in a tropical atmosphere ocean model: Influence of the basic state, ocean geometry and nonlinearity, *J. Atmos. Sci., 46,* 1687-1712, 1989.

Battisti, D. S., and E. S. Sarachik, Understanding and predicting ENSO, *Rev. Geophys., 33,* 1367-1376, 1995.

Betts, A. K., and W. Ridgway, Climatic equilibrium of the atmospheric convective boundary-layer over a tropical Ocean, *J. Atmos. Sci., 46,* 2621-2641, 1989.

Bjerknes, J., Atmospheric teleconnections from the equatorial Pacific, *Mon. Weather Rev., 97,* 163-172, 1969.

Blanke, B., and P. Delecluse, Low-frequency variability of the tropical Atlantic ocean simulated by a general circulation model with mixed layer physics, *J. Phys. Oceanogr., 23,* 1363-1388, 1993.

Boulanger, J.-P., and L. Fu, Evidence of boundary reflection of Kelvin and first-mode Rossby waves from TOPEX/Poseidon sea level data, *J. Geophys. Res., 101,* 16,361-16,371, 1996.

Boulanger, J.-P., and C. Menkes, Propagation and reflection of long equatorial waves in the Pacific Ocean during the 1992-1993 El Niño, *J. Geophys. Res., 100,* 25,041-25,059, 1995.

Boulanger, J. P., and C. Menkes, Long equatorial wave reflection in the Pacific Ocean from TOPEX/Poseidon data during the 1992-1998 period, *Clim. Dyn., 15,* 205-225, 1999.

Boutin J., et al., Satellite sea surface temperature: A powerful tool for interpreting in situ pCO_2 measurements in the equatorial Pacific Ocean, *Tellus, Ser. B, 51,* 490-508, 1999.

Cane, M. A., and R. J. Patton, A numerical model for low frequency equatorial dynamics, *J. Phys. Oceanogr., 14,* 1853-1863, 1984.

Chambers, D. P., B. D. Tapley, and R. H. Steward, Measuring heat storage changes in the equatorial Pacific: A comparison between TOPEX altimetry and Tropical-Atmosphere-Ocean buoys, *J. Geophys. Res., 103,* 18,591-18,597, 1998.

Chavez, F. P., and R. T. Barber, An estimate of new production in the Equatorial Pacific, *Deep Sea Res., Part A, 34,* 1229-1243, 1987.

Chen, D. K., L. Rothstein, and A. J. Busalacchi, A hybrid vertical mixing scheme and its application to tropical ocean models, *J. Phys. Oceanogr., 24,* 2156-2179, 1994.

Cheney, R. E., N. Doyle, B. C. Douglas, R. Agreen, L. Miller, E. Timmerman, and D. McAdoo, The complete GEOSAT altimeter GDR handbook, NOAA Rep., 79 pp., Natl. Oceanic and Atmos. Admin., Rockville, Maryland, 1991.

Clarke, A. J., Why are surface equatorial ENSO winds anomalously westerly under anomalous large-scale convection?, *J. Phys. Oceanogr., 7,* 1623-1627, 1994.

Clarke, A. J., J. Wang, and S. Van Gorder, A simple warm-pool displacement ENSO model, *J. Phys. Oceanogr., 30,* 1679-1691, 2000.

Cronin, M. F., and M. J. McPhaden, Upper ocean salinity balance in the western equatorial Pacific, *J. Geophys. Res., 103,* 27,567-27,587, 1998.

Dandonneau, Y., Seasonal or aperiodic cessation of oligotrophy in the tropical Pacific Ocean, *in Toward a Theory on Biological-Physical Interactions in the World Ocean,* edited by B. J. Rotchild, pp. 137-156, Kluwer Acad., New-York, 1988.

Delcroix, T., Observed surface oceanic and atmospheric variability in the tropical Pacific at seasonal and ENSO timescales: A tentative overview, *J. Geophys. Res., 103,* 18,611-18,633, 1998.

Delcroix, T., and J. Picaut, Zonal displacement of western equatorial Pacific "fresh pool," *J. Geophys. Res., 103,* 1087-1098, 1998.

Delcroix, T., G. Eldin, M.-H. Radenac, J. Toole, and E. Firing, Variations of the western equatorial Pacific Ocean, 1986-1988, *J. Geophys. Res., 97,* 5423-5447, 1992.

Delcroix, T., G. Eldin, M. McPhaden, and A. Morliere, Effects of westerly wind bursts upon the western equatorial Pacific Ocean, February-April 1991, *J. Geophys. Res., 98,* 16,379-16,385, 1993.

Delcroix, T., J.-P. Boulanger, F. Masia, and C. Menkes, Geosat-derived sea-level and surface-current anomalies in the equatorial Pacific, during the 1986-1989 El Niño and La Niña, *J. Geophys. Res., 99,* 25,093-25,107, 1994.

Delcroix, T., C. Hénin, V. Porte, and P. Arkin, Precipitation and sea-surface salinity in the tropical Pacific ocean, *Deep Sea Res., Part I, 43,* 1123-1141, 1996.

Delcroix, T., B. Dewitte, Y. du Penhoat, F. Masia, and J. Picaut, Equatorial waves and warm pool displacements during the 1992-1998 ENSO events: Observations and modeling, *J. Geophys. Res., 105,* 26,045-26,062, 2000.

Delecluse, P., G. Madec, M. Imbard, and C. Levy, OPA version 7: General Circulation Model reference manual, *Internal Rep. 93/05,* 140 pp.. Lab. d'Océanogr. Dyn. et de Climatol., Paris, France, 1993.

Deser, C., and J. M. Wallace, Large-scale atmospheric circulation features of warm and cold episodes in the tropical Pacific, *J. Clim., 3,* 1224-1281, 1990.

Dewitte, B., G. Reverdin, and C. Maes, Vertical structure of an OGCM simulation of the equatorial Pacific in 1985-1995, *J. Phys. Oceanogr., 29,* 1542-1570, 1999.

du Penhoat, Y., T. Delcroix, and J. Picaut, Interpretation

of Kelvin/Rossby waves in the equatorial Pacific from model-Geosat data intercomparison during the 1986-1987 El Niño, *Oceanol. Acta, 15,* 545-554, 1992.

Doulman, D. J., Development and expansion of the tuna purse seine fishery, *in Tuna Issues and Perspectives in the Pacific Islands Region.*, edited by D. J. Doulman, East-West Center, Univ. of Hawaii at Manoa, Honolulu, 133-160, 1987.

Eldin, G., M.-H. Radenac, and M. Rodier, Physical and nutrient variability in the upper equatorial Pacific associated with westerly wind forcing and wave activity in October 1994, *Deep-Sea Res., Part II, 44,* 1783-1800, 1997.

Feely, R. A., R. Wanninkhof, T. Takahashi, R. Wanninkhof, and P. Tans, Influence of El Niño on the equatorial Pacific contribution to atmospheric CO_2 accumulation, *Nature, 398,* 597-601, 1999.

Fonteneau, A., Atlas of tropical tuna fisheries, world catches and environment, *in ORSTOM Editions, Paris,* 192 pp., Institut de recherche pour le Développement, Paris, 1997.

Frankignoul, C., F. Bonjean, and G. Reverdin, Interannual variability of surface currents in the tropical Pacific during 1987-1993, *J. Geophys. Res., 101,* 3629-3647, 1996.

Fu, C., H. Diaz, and J. Fletcher, Characteristics of the response of sea-surface temperature in the central Pacific associated with warm episodes of the southern oscillation, *Mon. Weather Rev., 114,* 1716-1738, 1986.

Gadgil, S., P. V. Joseph, and N. V. Joshi, Ocean-atmosphere coupling over monsoon regions, *Nature, 312,* 141-143, 1984.

Geisler, J. E., M. L. Blackmon, G. T. Bates, and S. Munoz, Sensitivity of January climate response to the magnitude and position of equatorial Pacific sea surface temperature anomalies, *J. Atmos. Sci., 42,* 1037-1149, 1985.

Gent, P., and M. A. Cane, A reduced Gravity, primitive equation model of the upper equatorial ocean, *J. Comput. Phys., 81,* 444-480, 1989.

Gill, A. E., Changes in thermal structure of the equatorial Pacific during the 1972 El Niño as revealed by bathythermograph observations, *J. Phys. Oceanogr., 12,* 1373-1387, 1983.

Godfrey J. S., R. A. Houze, R. H. Johnson, R. Lukas, J.-L. Redelsperger, A. Sumi, and R. Weller R, Coupled Ocean-Atmosphere Response Experiment (COARE): An interim report, *J. Geophys. Res,., 103,* 14,395-14,450, 1998.

Graham, N. E., and T. P. Barnett, Sea surface temperature, sea surface wind divergence, and convection over tropical oceans, *Science, 238,* 657-659, 1987.

Graham, N. E., T. P. Barnett, and R. Wilde, On the roles of tropical and midlatitude SSTs in forcing interannual to interdecadal variability in the winter Northern Hemisphere circulation, *J. Clim., 7,* 1416-1441, 1994.

Guilderson, T. P., and D. P. Schrag, Abrupt shift in subsurface temperatures in the tropical Pacific associated with changes in El Niño, *Science, 2981,* 240-243, 1998.

Hansen D. V., and M. S. Swenson, Mixed layer circulation during EqPac and some thermochemical implications for the equatorial cold tongue, *Deep Sea Res., Part II, 43,* 707-724, 1996.

Harrison D. E., and N. K. Larkin, El Niño-Southern oscillation sea surface temperature and wind anomalies, 1946-1993, *Rev. Geophys., 36,* 353-399, 1998.

Hayes, S. P., L. J. Mangum, J. Picaut, A. Sumi, and K. Takeuchi, TOGA-TAO: A moored array for real-time measurements in the tropical Pacific Ocean, *Bull. Am. Meteorol. Soc., 72,* 339-347, 1991.

Hénin, C., and J. Grelet, A merchant ship thermosalinograph network in the tropical Pacific, *Deep-Sea Res., Part II, 43,* 1833-1855, 1996.

Hénin, C., Y. du Penhoat, and M. Ioualalen, Observations of sea-surface salinity in the western Pacific fresh pool: Large scale changes during 1992-1995, *J. Geophys. Res., 103,* 7523-7536, 1998.

Hirst, A. C., Slow instabilities in tropical ocean basin-global atmosphere models, *J. Atmos. Sci, 45,* 830-852, 1988.

Ho, C.-R., X.-H. Yan, and Q. Zheng, Satellite observations of upper-layer variabilities in the western Pacific warm pool, *Bull. Am. Meteorol. Soc., 76,* 669-679, 1995.

Hoerling, M. P., A. Kumar, and M. Zhong, El Niño, La Niña, and the nonlinearities of their teleconnections, *J. Clim., 10,* 1769-1786, 1997.

Inoue H. Y., M. Ishii, H. Matsueda, M. Ahoyama, and I. Asanuma, Changes in longitudinal distribution of the partial pressure of CO_2 (pCO_2) in the central and western equatorial Pacific, west of 160°W, *Geophys. Res. Lett., 23,* 1781-1784, 1996.

Kessler, W. S., M. J. McPhaden, and K. M. Weickmann, Forcing of intraseasonal Kelvin waves in the equatorial Pacific, *J. Geophys. Res., 100,* 10,613-10,631, 1995.

Kuroda, Y., and M. J. McPhaden, Variability in the western equatorial Pacific Ocean during Japanese Pacific Climate Study cruises in 1989 and 1990, *J. Geophys. Res., 98,* 4747-4759, 1993.

Lau, K.-M., and H. Weng, Interannual, decadal-interdecadal, and global warming signals in sea surface temperature during 1955-97, *J. Clim., 12,* 1257-1267, 1999.

Le Borgne, R., and M. Rodier, Net zooplankton and the biological pump: A comparison between the oligotrophic and mesotrophic equatorial Pacific, *Deep Sea Res., Part II, 44,* 2003-2023, 1997.

Le Borgne, R., M. Rodier, and G. Eldin, FLUPAC cruise focuses on ocean carbon cycle, *U. S. JGOFS Newsl.,* 9-11, January 1995.

Legler, D. M., and J. J. O'Brien, *Atlas of the Tropical Pacific Wind Stress Climatology 1971-1980,* 182 pp., Dep. of Meteorol., Florida State Univ., Tallahassee, 1984.

Lehodey P., M. Bertignac, J. Hampton, A. Lewis, and J. Picaut, El Niño Southern Oscillation and tuna in the western Pacific, *Nature, 389,* 715-718, 1997.

Lehodey, P., J.-M. Andre, M. Bertignac, J. Hampton, A. Stoens, C. Menkes, L. Memery, and N. Grima, Predicting skipjack tuna forage distributions in the equatorial Pacific using a coupled dynamical bio-geochemichal model, *Fish. Oceanogr., 7,* 317-325, 1998.

Lemasson, L., and B. Piton, Anomalie dynamique de la surface de la mer le long de l'équateur dans l'océan Pacifique, *Cah. ORSTOM, Ser. Oceanogr., 6,* 39-45, 1968.

Lindzen, R., and S. Nigam, On the role of sea surface temperature gradients in forcing low-level winds and convergence in the tropics, *J. Atmos. Sci., 44,* 2418-2436, 1987.

Liu, T., and C. Gautier, Thermal forcing on the tropical Pacific from satellite data, *J. Geophys. Res., 95,* 13,209-13,217, 1990.

Liu, W. T., A. Z. Zhang, and J. K. B., Bishop, Evaporation and solar irradiance as regulators of sea-surface temperature in annual and interannual changes, *J. Geophys. Res., 99,* 12,623-12,637, 1994.

Lukas, R., and E. Lindström, The mixed layer of the western equatorial Pacific Ocean, *J. Geophys. Res., 96,* 3343-3457, 1991.

Lukas, R., and P. Webster, TOGA-COARE, Tropical Ocean Global Atmosphere program and Coupled Ocean Atmosphere Response Experiment, *Oceanus, 35,* 62-65, 1992.

Maes, C., G. Madec, and P. Delecluse, Sensitivity of an equatorial Pacific OGCM to the lateral diffusion, *Mon. Weather Rev., 125,* 958-971, 1997.

Maes, C., P. Delecluse, and G. Madec, Impact of westerly wind bursts on the warm pool of the TOGA-COARE domain in an OGCM, *Clim. Dyn., 14,* 55-70, 1998.

Maes, C., D. Behringer, R. W. Reynolds, and M. Ji, Retrospective analysis of the salinity variability in the western tropical Pacific Ocean using an indirect minimization approach, *J. Atmos. Oceanic Technol., in press,* 2000.

Mangum, L. J., S. P. Hayes, J. M. Toole, Z. Wang, S. Pu, and D. Hu, Thermohaline structure and zonal pressure gradient in the western equatorial Pacific, *J. Geophys. Res., 95,* 7279-7288, 1990.

Mantua N. J., and D. S. Battisti, Evidence for the delayed oscillator mechanism for ENSO: The observed oceanic Kelvin mode in the far western Pacific, *J. Phys. Oceanogr., 24,* 691-699, 1994.

McCreary, J. P., Eastern tropical ocean response to changing wind systems with application to El Niño, *J. Phys. Oceanogr., 6,* 632-645, 1976.

McCreary, J. P., Equatorial beams, *J. Mar. Res., 42,* 395-430, 1984.

McPhaden, M., TOGA-TAO and the 1991-93 El Niño Southern Oscillation event, *Oceanog., 6,* 36-44,1993.

McPhaden, M. J., and J. Picaut, El Niño-Southern Oscillation displacement of the western equatorial Pacific warm pool, *Science, 250,* 1385-1388, 1990.

McPhaden, M. J., and B. A. Taft, On the dynamics of seasonal to intraseasonal variability in the eastern equatorial Pacific, *J. Phys. Oceanogr., 18,* 1713-1732, 1988.

McPhaden, M. J., and J. Yu, Equatorial waves and the 1997-98 El Niño, *Geophys. Res. Lett., 26,* 2961-2964, 1999.

McPhaden M. J., F. Bahr, Y. du Penhoat, E. Firing, S. P. Hayes, P. P. Niiler, P. L. Richardson, and J. M. Toole, The response of the western equatorial Pacific Ocean to westerly wind bursts during November 1989 to January 1990, *J. Geophys. Res., 97,* 14,289-14,303, 1992.

McPhaden, M. J., et al., The tropical ocean global atmosphere observing system: A decade of progress, *J. Geophys. Res., 103,* 14,169-14,240, 1998.

Murtugudde, R. G., and A. J. Busalacchi, Salinity effects in a tropical ocean model, *J. Geophys. Res., 103,* 3283-3300, 1998.

Murtugudde, R. G., S. R. Signorini, J. R. Christian, A. J. Busalacchi, C. R. McLain, and J. Picaut, Ocean color variability of the tropical Indo-Pacific basin observed by SeaWiFS during 1997-98, *J. Geophys. Res., 104,* 18,351-18,366, 1999.

Neelin, J. D., D. S. Battisti, and A. C. Hirst, ENSO theory, *J. Geophys. Res., 103,* 14,261-14,290, 1998.

Palmer, T., and D. Mansfield, Response of two atmospheric general circulation models to sea surface temperature anomalies in the tropical east and west Pacific, *Nature, 310,* 483-485, 1984.

Perigaud, C., and B. Dewitte, El Niño-La Niña events simulated with Cane and Zebiak's model and observed with satellite or in situ data, part I: Model data comparison, *J. Clim., 9,* 66-84, 1996.

Philander, S. G. H., *El Niño, La Niña, and the Southern Oscillation,* 293 pp., Academic, San Diego, Calif., 1990.

Philander, S. G. H., and R. C. Pacanowski, The generation of equatorial currents, *J. Geophys. Res., 85,* 1123-1136, 1980.

Picaut, J., and R. Tournier, Monitoring the 1979-1985 equatorial Pacific current transports with expendable bathythermograph data, *J. Geophys. Res., 100,* 3263-3277, 1991.

Picaut, J., and T. Delcroix, Equatorial wave sequence associated with the warm pool displacement during the 1986-1989 El Niño and La Niña, *J. Geophys. Res., 96,* 18,398-18,408, 1995.

Picaut, J., A. J. Busalacchi, M. J. McPhaden, and B. Camusat, Validation of the geostrophic method for estimating zonal currents at the equator from Geosat altimeter data, *J. Geophys. Res., 95,* 3015-3024, 1990.

Picaut, J., M. Ioualalen, C. Menkes, T. Delcroix, and M. J. McPhaden, Mechanism of the zonal displacements of the Pacific Warm Pool, implications for ENSO, *Science, 274,* 1486-1489, 1996.

Picaut, J., F. Masia, and Y. du Penhoat, An advective-reflective conceptual model for the oscillatory nature of the ENSO, *Science, 277,* 663-666, 1997.

Poulain, P. M., Estimates of horizontal divergence and vertical velocity in the equatorial Pacific, *J. Phys. Oceanogr., 23,* 601-607, 1993.

Ralph, E. A., K. Bi, P. P. Niiler, and Y. du Penhoat, A Lagrangian description of the western equatorial Pacific response to the wind burst of December 1992, *J. Clim., 10,* 1706-1721, 1997.

Reverdin, G., C. Frankignoul, E. Kestenare, and M. J. McPhaden, A climatology of the seasonal currents in the equatorial Pacific, *J. Geophys. Res., 99,* 20,323-20,344, 1994.

Reynolds, D., and T. Smith, Improved global sea surface temperature analyses using optimum interpolation, *J. Clim., 7,* 929-948, 1994.

Roemmich, D., M. Morris, W. R. Young, and J.-R. Donguy, Fresh equatorial jets, *J. Phys. Oceanogr., 24,* 540-558, 1994.

Schneider, E. K., B. Huang, and J. Shukla, Ocean wave dynamics and El Niño, *J. Clim., 8,* 2415-2439, 1995.

Schneider N., T. Barnett, M. Latif, and T. Stockdale, Warm pool physics in a coupled GCM, *J Clim., 9,* 219-239, 1996.

Schopf, P. S., and M. J. Suarez, Vacillations in a coupled ocean-atmosphere model, *J. Atmos. Sci., 45,* 549-566, 1988.

Seager, R., M. Blumenthal, and Y. Kushnir, An advective atmospheric mixed layer model for ocean modeling purposes; Global simulation of surface heat fluxes, *J. Clim., 8,* 1951-1964, 1995.

Smith, T. M., R. W. Reynolds, R. E. Livezey, and D. C. Stokes, Reconstruction of historical sea surface temperature using empirical orthogonal functions, *J. Climate, 9,* 1403-1420, 1996.

Shinoda, T., and R. Lukas, Lagrangian mixed layer modelling of the western equatorial Pacific, *J. Geophys. Res., 100,* 2523-2541, 1995.

Sprintall, J., and M. J. McPhaden, Surface layer variations observed in multiyear time series measurements from the western equatorial Pacific, *J. Geophys. Res., 101,* 22,513-22,533, 1994.

Sprintall, J., and M. Tomczak, Evidence of the barrier layer in the surface layer of the tropics, *J. Geophys. Res., 97,* 7305-7316, 1992.

Stoens A., et al., The coupled physical-new production system in the equatorial Pacific during the 1992-1995 El Niño, *J. Geophys. Res., 104,* 3323-3339, 1999.

Trenberth, K., and T. Hoar, The 1990-1995 El Niño-Southern Oscillation event: Longest on record, *Geophys. Res. Lett., 23,* 57-60, 1996.

Vialard, J., and P. Delecluse, An OGCM study for the TOGA decade, part I, Role of salinity in the physics of the western Pacific fresh pool, *J. Phys. Oceanogr., 28,* 1071-1088, 1998a.

Vialard, J., and P. Delecluse, An OGCM study for the TOGA decade, part II, Barrier-layer formation and variability, *J. Phys. Oceanogr., 28,* 1089-1106, 1998b.

Vialard, J., C. Menkes, J.-P. Boulanger, P. Delecluse, E. Guilyardi, M. J. McPhaden, and G. Madec, A model study of oceanic mechanisms affecting equatorial sea surface temperature during the 1997-98 El Niño, *J. Phys. Oceanogr.,* in press, 2000.

Wallace, J. M., Effect of deep convection on the regulation of tropical sea surface temperature, *Nature, 357,* 230-231, 1992.

Wang, W., and M. J. McPhaden, The surface layer heat balance in the equatorial Pacific Ocean, part II, Interannual variability, *J. Phys. Oceanogr.*, in press, 2000.

Webster, P. J., and R. Lukas, TOGA-COARE: The Coupled Ocean Atmosphere Response Experiment, *Bull. Am. Meteorol. Soc., 9,* 1377-1416, 1992.

Wu, Z., E. S. Sarachik, and D. S. Battisti, Thermally forced surface winds on an equatorial beta-plane, *J. Atmosph. Sci., 56,* 2029-2037, 1999.

Wyrtki, K., El Niño - the dynamic response of the equatorial Pacific ocean to atmospheric forcing, *J. Phys. Oceanogr., 5,* 572-584, 1975.

Wyrtki, K., The slope of sea level along the equator during the 1982-83 El Niño, *J. Geophys. Res., 89,* 10,419-10,424, 1984.

Wyrtki, K., Water displacements in the Pacific and the genesis of El Niño cycles, *J. Geophys. Res., 90,* 7129-7132, 1985.

Xie, P., and P. Arkin, Analyses of global monthly precipitation using gauge observations, satellite estimates, and numerical model predictions, *J. Clim., 9,* 840-858, 1996.

Yan, X.-H., Y. He, W. T. Liu, Q. Zheng, and C.-H. Ho, Centroid movement of the western Pacific warm pool during the three recent El Niño-Southern Oscillation events, *J. Phys. Oceanogr., 27,* 837-845, 1997.

Yang, S., K.-M. Lau, and P. S. Schopf, Sensitivity of the tropical Pacific Ocean to precipitation-induced freshwater flux, *Clim. Dyn., 15,* 737-750, 1999.

Yoder J. A., S. G. Ackleson, R. T. Barber, P. Flament, and W. M. Balch, A line in the sea, *Nature, 371,* 689-692, 1994.

You, Y., Salinity variability and its role in the barrier layer formation during TOGA-COARE, *J. Phys. Oceanogr., 25,* 2778-2807, 1995.

Zebiak, S. E., and M. A. Cane, A model of El Niño Southern Oscillation, *Mon. Weather Rev., 115,* 2262-2278, 1987.

T. Delcroix, F. Masia and M. Ioualalen, Centre IRD de Nouméa, B.P. A5, 98848 Nouméa Cedex, New-Caledonia.

R. Murtugudde, Earth System Science Interdisciplinary Center, University of Maryland, College Park, MD 20742.

J. Picaut, IRD-LEGOS, 18 av. Edouard Belin, 31401 Toulouse cedex 4, France. (Joel.Picaut@cnes.fr)

J. Vialard, European Centre for Medium-range Weather Forecasts, Shinfield Park, Reading, Berkshire RG2 9AX, England, United Kingdom.

(Received July 13, 1999; revised June 29, 2000;
accepted August 12, 2000.)